

GLD224

THE TUSCARORA, NEVADA GEOTHERMAL PROSPECT

A Continuous Case History

PART I (Text)

by Frederick E. Berkman

*Paper delivered at the Fiftieth Annual Meeting
of the Society of Exploration Geophysicists,
Houston, Texas, 17 November 1980.*

AMAX Exploration Inc.
Geothermal Branch
7100 W. 44th Avenue
Wheat Ridge, Colorado 80033

THE TUSCARORA, NEVADA GEOTHERMAL PROSPECT

A Continuing Case History (Abstract)

by Fred Berkman, AMAX Exploration Inc., Geothermal Branch

The Tuscarora prospect is located in northeastern Nevada, 100 km north-northwest of Elko. Exploration is being conducted by AMAX Exploration, Inc., as a participant in the Department of Energy's Industry-Coupled Geothermal Program. Earth Power Production Company of Tulsa and Supron Energy of Dallas are partners with AMAX in this venture.

The geothermal area occurs along the north end of the Independence Valley graben. This basin-range structure seems to terminate where it abuts the Snake River downwarp. As the basin/range faults intersect the Snake River downwarp they are severely offset within a zone of northeast-trending left-lateral faults known as the Midas trench. East of this graben, the Independence Mountains which contain a thick sequence of Paleozoic limestones, siltstones and quartzites. Within the Midas Trench are extensive exposures of Tertiary rocks--stream and lake sediments with tuffs, ignimbrites and minor volcanic flows. Quaternary terrace gravels and alluvium conveniently hide many of the transgraben faults.

Thermal manifestations include 6 springs, 20 hot springs, one geyser and one fumerole. These occur in a narrow zone approximately 3 km long within the Midas fault zone. Waters from the hot springs were analyzed and subsurface temperatures of 228°C and 167°C were indicated by the Na-K-Ca and silica geothermometers.

Data collected in 38 temperature gradient holes from 40 to 610m deep, showed an irregularly shaped thermal anomaly centered just north of the graben-trench intersection. Approximately 20km² (5000 acres) lies within the 10 HFU contour.

The complete Bouguer gravity data show a 15 milligal low over the northern Independence Valley. A series of smaller connected lows extend to the north and northwest across the Midas Trench. The gravity gradients indicate three well developed fault sets trending north-south, northeast-southwest and northwest-southeast.

An aeromagnetic survey flown approximately 1km above the topography (2.74km CBA) indicates structural subsidence and possible doming within the Midas Trench. It also indicates the presence of several intrusives peripheral to the heatflow anomaly. Preliminary inversions indicate a possible zone of hydrothermal alteration coincident with the hot spring trend.

Passive seismic monitoring recorded 108 events during a 12-day period. Magnitudes ranged from 0.5 and 2.4. Depths ranged from 3 to 13km. Most epicenters were located along the eastern margin of the Independence Valley near the graben-trench intersection. A zone of P-wave delay occurs beneath the north end of Independence Valley.

Three electrical techniques were used. Self-potential measurements were made along eight east-west profiles. They show a transition from positive to negative readings across the graben-trench intersection. Other SP anomalies are probably related to graphitic rocks in the Valmy formation and mapped sulfide occurrences.

A dipole-dipole resistivity survey was conducted using a dipole separation of 610 meters and a N spacing of 5. All three profile lines exhibited a resistor over conductor configuration. Resistivities less than 8 ohmmeters characterized the conductive zone which coincided with the center of the heatflow anomaly. Range front faults appear to be well defined by moderate resistivity contrasts.

Magnetotelluric stations were located along the dipole-dipole profiles lines. Data were recorded at 30 stations over a frequency band of .01 to 10Hz and inverted to depth sections using the Bostick inversion. The MT survey revealed two major conductors. One is the shallow conductor seen by the resistivity survey. The second conductor ($1 \Omega m$) occurs below 5km in a north-south trending zone at the north end of the Independence Valley. This zone correlates with moderate heatflow, fault intersections, microearthquakes, gravity lows, an SP high and a zone of P-wave delay.

A deep (1663-meter) test near the hot springs failed to encounter a reservoir. Information from the well has been helpful in clarifying the thermal regime and in locating a second deep well.

INTRODUCTION

(SLIDE 1L & 2R) My talk this morning is on the Tuscarora geothermal prospect located in northeastern Nevada approximately 90km northwest of Elko. Initial interest in the prospect was based on a 216⁰C geothermometer temperature obtained from reconnaissance sampling during the Summer 1977. Exploration is being conducted by AMAX Exploration, Inc. as a participant in the Department of Energy, Industry-coupled geothermal program. Earth Power Production Company of Tulsa and Supron Energy of Dallas are partners with AMAX in this venture.

In my talk today I will be discussing the results of heatflow, self-potential, gravity, magnetics, passive seismic, resistivity and MT surveys. Since in many ways this prospect is typical of Basin /Range geothermal systems, this discussion may be helpful in indicating the effectiveness of the various geophysical techniques for this type of prospect. I would like to thank the DOE, Earth Power Production Company, Supron Energy and AMAX Exploration for the permission and opportunity to present these interim results.

LOCATION AND DESCRIPTION

(SLIDE 2R) This slide, looking east, shows the upper hot springs. The middle dark hill is a dacite intrusion. Independence Valley lies between the intrusion and the snow-covered Independence Mtns in the background.

(SLIDE 3L) The prospect comprises approximately 121km² in the low rolling hills at the north end of the Independence Valley. Thermal manifestations include 6 warm springs, 20 hot springs, one geyser and one fumarole. Elevation varies from 2.6km (8600ft) in the Independence and Tuscarora Mtns to 1.7km (5600ft) in the Independence Valley. The direction of surface water drainage is generally south into the Owyhee River which flows to the northwest. The mines shown produced silver and gold.

The blue arrow shows the location of the deep test well. The hole bottomed in metasediments at 1.6km (5300ft). The deepest calculated equilibration temperature was 135⁰C at 1.2km (4100ft). An oil and gas test (Ellison #1) was drilled here. It bottomed in volcanoclastics at 1.3km. (Deep DH; oil and gas)

GEOLOGY

(SLIDES 4L & 5R) The geology can be simply divided into three main units (Pilkington, 1979). The Independence Mtns are composed of Paleozoic sedimentary rocks probably greater than 3km thick--quartzites, siltstones and cherts with minor limestones, conglomerates and volcanics.

The Tertiary rocks in the Tuscarora area are a sequence of intercalated sediments, tuffs and minor volcanic flows up to 1.5km thick. The youngest Tertiary rocks are volcanics varying from andesite to rhyolite in composition and from 6-17 million years in age. Quaternary alluvium covers the Independence Valley.

A complicated tectonic history is indicated. Thrusting pushed the eugeosynclinal western facies rocks eastward over the miogeosynclinal rocks. East-west extension produced in the N/S-trending basin/range structures, such as the fault-bounded Independence Valley.

The basin/range structures are offset by two sets of strike-slip faults. The northeast trending left-lateral faults are part of the Midas Trench lineament system. The second set are right lateral faults which trend northwestward and become the dominant structural grain northward into the Owyhee uplift. Movement along these conjugate shear directions began 15 million years ago and continues today.

(SLIDE 5R) This slide shows an east/west geologic section. The essential elements to keep in mind as I cover the geophysics are: 1) the intrusions at the Hot Springs and along the east valley margin; 2) the structural high at the Hot Springs; and 3) the Midas strike-slip and basin/range normal faults.

GEOCHEMISTRY

(SLIDE 6L) In terms of its geochemical attributes, the sodium bicarbonate waters issue from the Hot Spring at a temperature of 90°C . By employing the silica and Na/K geochemical thermometers, and assuming 54% cold water mixing, we obtain temperatures of last equilibration of 167° and 227° , respectively, (Dellechaie, 1977) suggestive of a high temperature reservoir.

Mercury in the soil, as seen in this profile, exhibits a 110 ppb high, over the thermal zone. The 40ppb background is a characteristic signature of young volcanics.

(SLIDE 7R) This slide shows a small hot pool in the lower hot springs group.

TEMPERATURE & HEATFLOW

(SLIDE 8L & 9R) The thermal data at Tuscarora, seen in the next slides, are the strongest geophysical evidence for a significant geothermal system. The thermal anomaly is based on temperature and thermal conductivity data collected from 38 drill holes which range from 40 to 522 meters deep. The anomaly is irregularly circular and occurs at the intersection of the Independence Valley graben and the Midas Trench. Two distinct peaks, 39 and 34HFU, about 2km apart, are separated by an east northeast zone of slightly lower heatflow. The heatflow low to the SE indicates cold water recharge.

(SLIDE 9R) Examining the thermal data along Profile A-A', we have constructed isotherms by linear extrapolation from measured gradients assuming conductive heat flow, not to be confused with formal downward continuation (this is the 100⁰C isotherm). A sharp heatflow high extends about 1km east of the hot springs across the dacite intrusion shown earlier. There is also a subtle hint of shallowing isotherms east of Harrington Creek which does not show on the heatflow curve. Also shown is the corresponding SP profile, which we will return to shortly.

(SLIDE 10R) Profile B-B' shows two curves immediately above the isotherms. The upper curve is the heatflow curve and the lower is the temperature at 100 meters. Both curves show the same pattern. The peak is 35 HFU. A broad (1.5km) thermal anomaly is centered just east of the hot springs, with a smaller anomaly west of Harrington Creek. The area 1km east or southeast of the Hot Springs on both profiles appears to be an attractive drilling target.

SELF POTENTIAL

(SLIDE 11L) We next examine the results of a detailed self-potential survey carried out by Microgeophysics Corporation along E-W grid lines. As Art Lange indicated in his talk, we face the interpretation problem with SP data of distinguishing between thermoelectric, electrokinetic and electrochemical causes (Corwin and Hoover, 1979). There is, as you can readily see, no prominent SP anomaly relating to the thermal anomaly or hot springs. The dominant feature in this slide is the regional decrease in voltage from +25mv in the southeast to -30mv in the northwest, which could be related to the Midas trend. A local 40mv decrease near the Spanish Ranch may be related to descending cold water. The strongest SP anomaly, a 0.4 volt low east of Jack Creek Lodge, may be caused by sulfide mineralization or a graphitic shale contact along the range front faults.

(SLIDE 10R) There is, however, a weak positive SP anomaly on Profile B-B' near the hot springs which is probably due to ascending hot fluids. The smaller anomaly west of Harrington Creek may be due to the same mechanism operating deeper in the section.

(SLIDE 12R) Similarly, on Profile A-A', a positive SP anomaly occurs over the heat flow high.

GRAVITY

(SLIDE 13L) We next examine the results of a gravity survey conducted by Microgeophysics Corp. As seen in this next slide, the complete Bouguer map shows a central low flanked by highs to the east and west. The lows occur over areas with thick sections of low density volcanoclastic rocks (2.2gm/cc). Basin margin faults are well indicated by high gradients. A small 5 milligal gravity high immediately north of the hot springs is thought to be a small horst possibly related to the intrusion near the hot springs.

(SLIDE 14R) The eastwest profile A-A' is located just north of the hot springs. Assuming that the local gravity features are primarily caused by low-density volcanoclastics overlying denser Paleozoic sediments, I have computed a 2-D depth section which has been constrained by surface geology and well control. Two positive anomalies indicate likely horsts, one below the hot spring and one 3.5km west. Interpreted faults are shown as well.

(SLIDE 15R) This slide shows the northwest/southeast profile B-B', which extends across the local high north of the hot springs. Interpreted faults possibly related to the Midas trend are more clearly shown south east of the hot springs. The volcanoclastic section appears to be about 2km thick at this point in the valley and dips to the southeast from the high near the hot springs.

The gravity data thus serve to elucidate structural elements and to estimate the thickness of Tertiary volcanoclastics.

MAGNETICS

(SLIDE 16L & SLIDE 17R) The next two slides show the results of an aeromagnetic survey flown at 2740m (9000 ft) by Geometrix. The data, after IGRF removal, have been color contoured at an interval of 25 gammas. The general pattern is considerably different than the gravity, partly because the Tuscarora mountains are covered with strongly magnetic volcanics and the Independence mountains are not. The Midas structure is evident as a weak but persistent northeast-trending gradient.

(SLIDE 17R) Some of the larger anomalies are intrusions, while surface flows with strong reversed remanent magnetizations account for the other local anomalies. These features are all fairly shallow, within a km of the surface. As with the gravity and SP, there is no magnetic anomaly directly relatable to the thermal feature.

(SLIDE 17Ra) Profile A-A' shows the ground mag, aeromag and a first iteration depth to magnetic basement. We see a weak magnetic low at the hot springs. The paleozoic contact occurs just east of Harrington Creek where the magnetic profiles become flat.

POISSON'S RATIO

(SLIDE 18L & Blank Right) In the next slide we see the results of a 11-day passive seismic survey conducted by Microgeophysics Corporation using a 15 station detector array. Epicenters are shown by the dots. A one-day swarm produced 103 of the 108 total events, indicating sporadic seismicity. A magnitude 2.44 earthquake occurred at the northeast corner of the Independence Valley. The hypocenters varied from 3 to 14km deep. Most of the activity appears to occur at the range front Midas Trench fault intersection. The high Poisson's Ratio (.35) is primarily influenced by the basin sediments and the low Poisson's Ratio (.20) by the rigid metasedimentary rocks such as occur in the Independence Range. None of the passive seismic survey can be related to the thermal feature.

DIPOLE-DIPOLE RESISTIVITY

(SLIDE 19L & 20R) The next slides show the results of a dipole-dipole resistivity survey performed by Mining Geophysical Surveys using 610 meter dipoles with maximum dipole separation of 5. Resistivities for $n=2$ are shown in plan view. We are seeing the averaged resistivities of approximately the upper 500 meters of section. A broad, well-defined low ($6-10\ \Omega\ m$) resistivity zone occurs at the north end of Independence Valley. Resistivities increase to the east and west, becoming most resistive ($900\ \Omega\ m$) over the metasediments exposed in the Independence Range.

(SLIDE 20R) The upper section in this slide is the observed apparent resistivity pseudosection. The lower section is a smoothed 2-D model which yields a fairly good fit to the observed data. The pseudosections were modelled by Claron Mackelprang from University Utah Research Institute. The orange represents the low resistivity zone less than 8 ohmmeters. This zone, encountered in the upper 400m of the deep test, corresponds to a sequence of volcanics, siltstones and shales moderately altered to clays with measured resistivities between 1 and $5\ \Omega\ m$. The maximum calculated equilibrium temperature of 147° was obtained immediately below this zone but above the resistive metasedimentary section. The low resistivity zone on the modelled section appears to be an alteration cap above the possible reservoir. On this section the conductive zone has an easterly dip. A more resistive (35 to $50\ \Omega\ m$) surface layer covers the conductor on the east. This shallow resistive layer corresponds to the surface volcanic flows and intrusions postulated as causing the previously shown magnetic anomalies.

(SLIDE 21R - Section B-B') B-B' is much the same, except that the low resistivity zone appears more extensive at depth. Note that we cannot see below the conductive zone with this dipole-dipole survey.

MAGNETOTELLURICS

(SLIDE 22L) The final data set, seen in the next slides, is a tensor magnetotelluric survey carried out by Terraphysics using the same remote reference field procedure described previously by Art Lange. Base stations are shown by colored squares. Satellite electric dipole pairs telemetered back to the base and used as remote reference signals for noise reduction are shown as circles. Data were obtained over a wide frequency band from 0.01 to 10Hz. Terraphysics converted the curves of tensor impedances vs. frequency at each station to profiles of resistivity vs. depth using the Bostick 1D inversion (Bostick, 1977). As you are aware, this inversion is only a first pass and large lateral discontinuities at basin margins seriously distort the resistivity picture.

(SLIDE 23L) Examining the data in plan form at a depth of 3km, we see that there are two conductive anomalies: one north of the Jack Creek Lodge, the other south of the Spanish Ranch. However, in the vicinity of the hot springs we observe generally intermediate resistivities at a depth of 3km. A zone of intermediate resistivities (64-128 Ω m) trends northeasterly and is probably related to the Midas Trench.

(SLIDE 24R) I would like to point out that the shallow conductive zone is indicated by both the dipole-dipole and MT survey. Below that, the MT indicates some highly resistive areas not seen by the dipole survey. This picture was reinforced during drilling when an increasingly resistive section (200-500 Ω m) of quartzites and dolomites was encountered in the bottom of 500 meters of hole. There is a suggestion of a conductive conduit at depth under the hot springs.

(SLIDE 25R) An additional conductivity conduit occurs in the vicinity of the Midas Trench faults shown previously. The deep conductive zone at the south/east end of the profile may be related to a source of volcanics at the valley margin.

(SLIDE 26L) Synthesizing the data, we see support for a shallow reservoir with a conductive cap on the dipole-dipole profiles and the upper MT section. This reservoir falls mostly within the heatflow anomaly. The possible deep heat sources are the conductors in the deeper part of the MT section.

(SLIDE 27R) Profile A-A' shows the reservoir as suggested by the data sets. The concept here is that the reservoir, principally defined by the dipole-dipole survey, is being recharged by descending surface water along the valley margin faults. We may speculate that heat is supplied to this system from a deep source which may be magmatic. Hot fluids generally circulate updip beneath the volcanoclastics with some minor leakage at the hot springs.

CONCLUSION

I conclude that heatflow, dipole-dipole resistivity and MT were the techniques which conveyed the most information about the prospect. Gravity, yielded some useful structural information. The SP, magnetics, and passive seismic were helpful mostly when used with the other data sets, but did not directly outline a reservoir. Finally AMAX is continuing to explore this promising prospect with a second deep test.

REFERENCES

- CORWIN, R.F., D.B. Hoover (1979). The self-potential method in geothermal exploration. *Geophysics* 44 (2). p. 226-245.
- DELLECHAIE, F. (1979). Hydrogeochemistry of the Tuscarora, Nevada, geothermal prospect. I.O.M.
- PILKINGTON, H.D. (1979). Geology of the Tuscarora Unit Area, Nevada. AMAX Exploration Inc. 9p, 9pl.
- BOSTICK, F.X. Jr. (1977). A simple almost exact method of MT analysis, v.s. Geology Survey work shop on electrical method in geothermal exploration at Snowbird, Utah. November 4-7, 1976.

CONTRACTOR REPORTS

- MICROGEOPHYSICS CORP. (1979). *Self-potential Survey, Tuscarora, Nevada*. Report prepared for AMAX Exploration Inc. 30 July 1979.
- MICROGEOPHYSICS CORP. (1980). *Tuscarora, Nevada Gravity Survey*. Report prepared for AMAX Exploration Inc. 11 January 1980.
- MICROGEOPHYSICS CORP. (1979). *Tuscarora Seismicity*. Report prepared for AMAX Exploration Inc. March 1979.
- MINING GEOPHYSICAL SURVEYS (1979). *Resistivity Survey, Tuscarora Project, Elko County, Nevada*. Report prepared for AMAX Exploration Inc. 17 August 1979.
- TERRAPHYSICS (1979). *Telluric-Magnetotelluric Survey at Tuscarora Prospect*. Report prepared for AMAX Exploration Inc. November 1979.

THE TUSCARORA, NEVADA GEOTHERMAL PROSPECT

A Continuous Case History

PART III (PLATES)

by Frederick E. Berkman

*Paper delivered at the Fiftieth Annual Meeting
of the Society of Exploration Geophysicists,
Houston, Texas, 17 November 1980.*

AMAX Exploration Inc.
Geothermal Branch
7100 W. 44th Avenue
Wheat Ridge, Colorado 80033

THE TUSCARORA, NEVADA GEOTHERMAL PROSPECT

A Continuous Case History

PART II (FIGURES)

by Frederick E. Berkman

*Paper delivered at the Fiftieth Annual Meeting
of the Society of Exploration Geophysicists,
Houston, Texas, 17 November 1980.*

AMAX Exploration Inc.
Geothermal Branch
7100 W. 44th Avenue
Wheat Ridge, Colorado 80033

FIGURES

- 1L. Location of Tuscarora prospect within state of Nevada.
- 2R. View of the upper hot springs with dacite intrusion in the middle ground and the Independence Range in the background.
- 3L. Orientation map showing principal features of the Tuscarora prospect.
- 4L. Simplified geologic map, showing out crop of Paleozoic rocks and Tertiary volcanics Quaternary alluvium and hot spring sinter (Pilkington, 1979).
- 5R. East-west geologic x-section 0.5 mile south of well 66-5 (Pilkington, 1979) showing intrusions and arched paleozoic rock beneath Tertiary volcanoclastics.
- 6L. Soil mercury profile and profile location.
- 7R. View of small hot pool in the lower hot springs group.
- 8L. Heatflow map showing profile locations.
- 9R. East-west heatflow profile A-A' showing isotherms and SP anomaly.
- 10R. Northwest-southeast heatflow profile B-B' showing temperature at 100 meters (curve just above isotherms) isotherms and SP anomaly.
- 11L. Self-potential map showing profile locations.
- 12R. Self-potential profiles A-A' and B-B'.
- 13L. Complete Bouguer gravity map.
- 14R. East-west gravity profile A-A' and depth section.
- 15R. Northwest-southeast profile B-B' and depth section.
- 16L. Residual magnetic map.
- 17R. Magnetic interpretation and profile A-A' location.
- 17Ra. Magnetic profile A-A' showing ground magnetics, aeromagnetics and depth to magnetic basement.
- 18L. Map of Poisson's Ratio and earthquake epicenters.
- 19L. Dipole-dipole resistivity for N=2 and A=610 meters showing profile locations.

- 20R. Resistivity section A-A' showing observed apparent resistivity pseudosection and modelled resistivity section.
- 21R. Resistivity section B-B' showing observed apparent resistivity pseudosection and modelled resistivity depth section.
- 22L. Magnetotelluric stations and profile location map.
- 23L. Resistivity at 3km from 1-D magnetotelluric inversion.
- 24R. MT resistivity section (T_e mode) along profile A-A'.
- 25R. MT resistivity section (T_e mode) along profile B-B'.
- 26L. Reservoir concept showing profile A-A' location.
- 27R. Geophysical synthesis and possible reservoir section along A-A'.

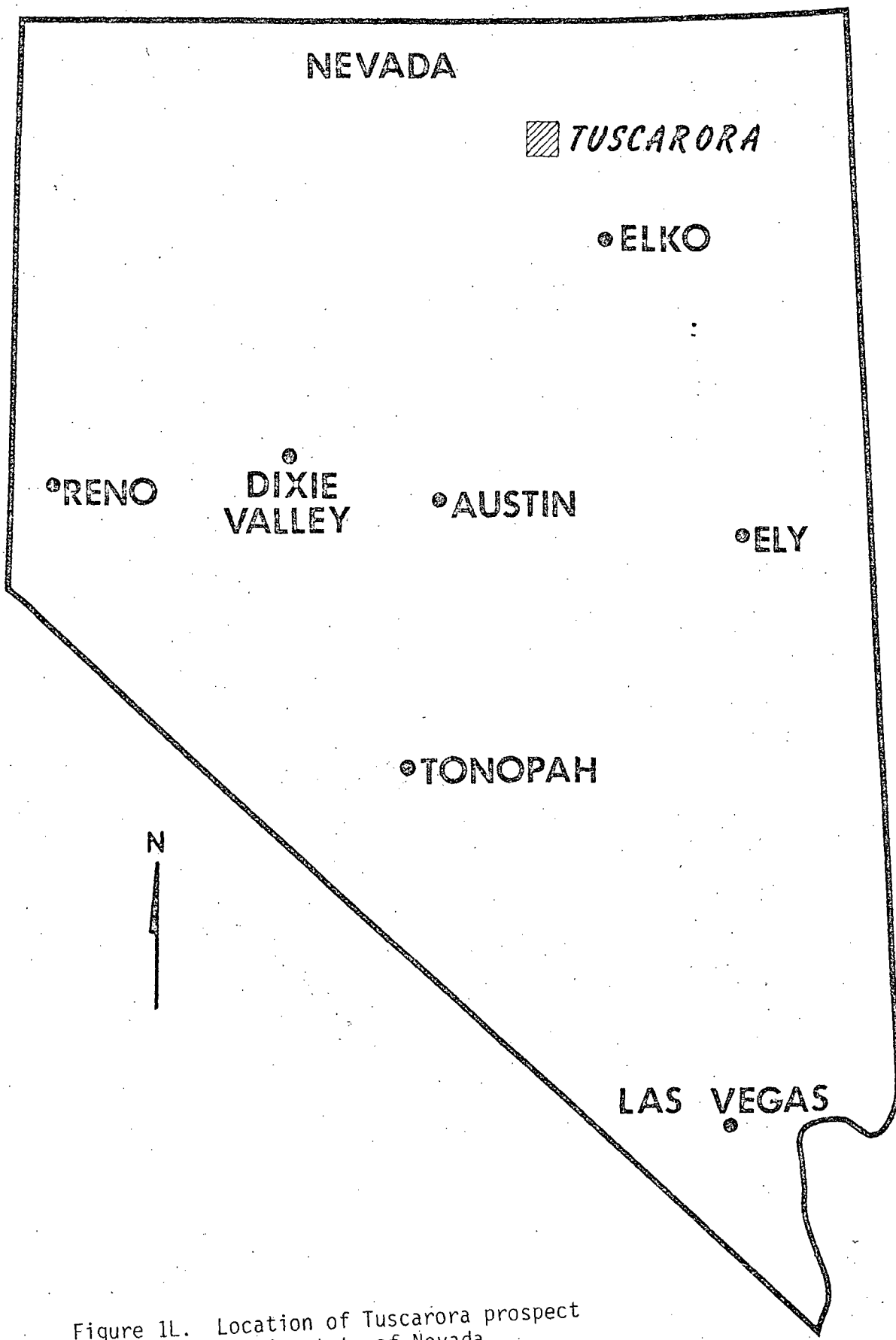


Figure 1L. Location of Tuscarora prospect within state of Nevada.

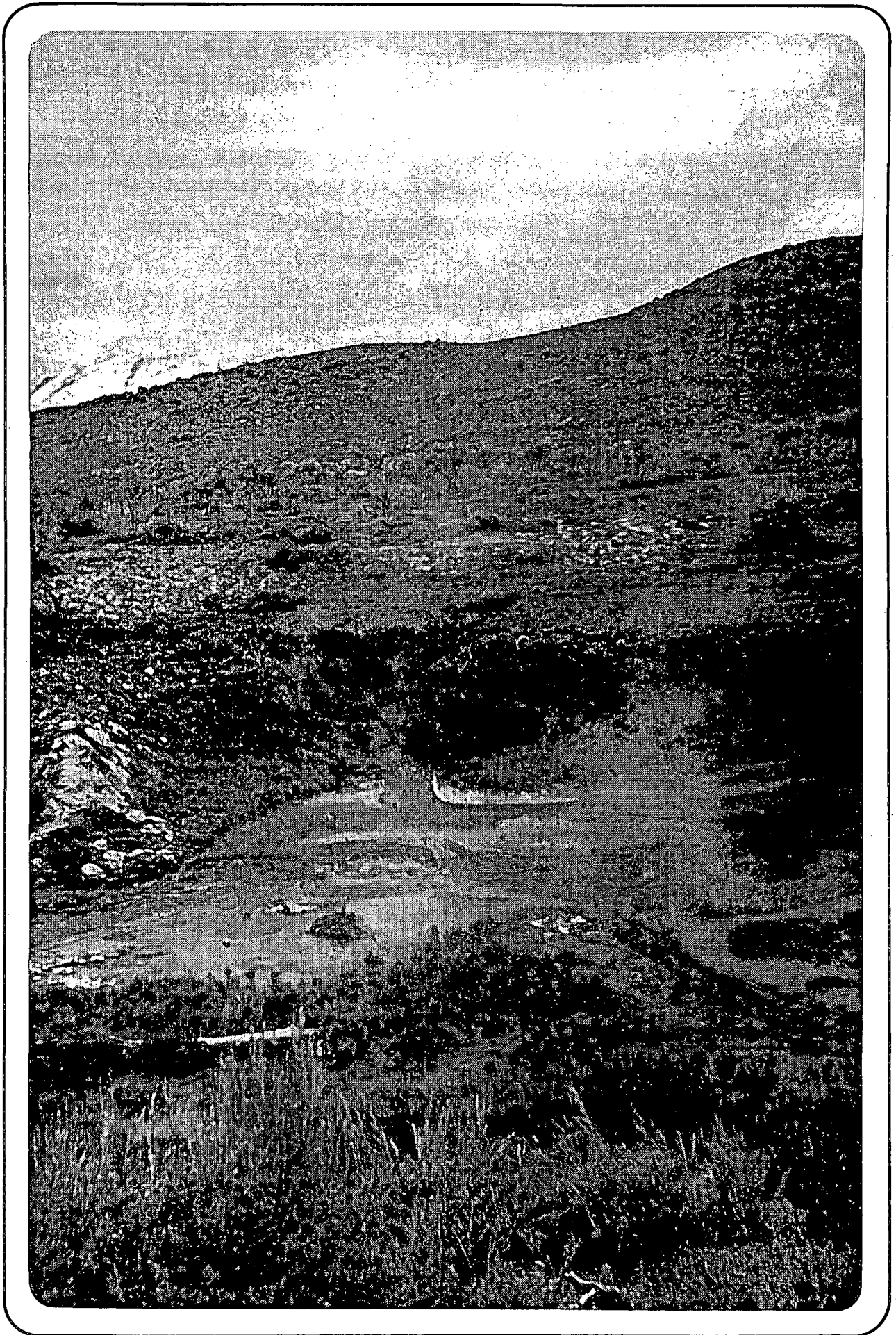


Figure 2R. View of the upper hot springs with dacite intrusion in the middle ground and the Independence Range in the background.

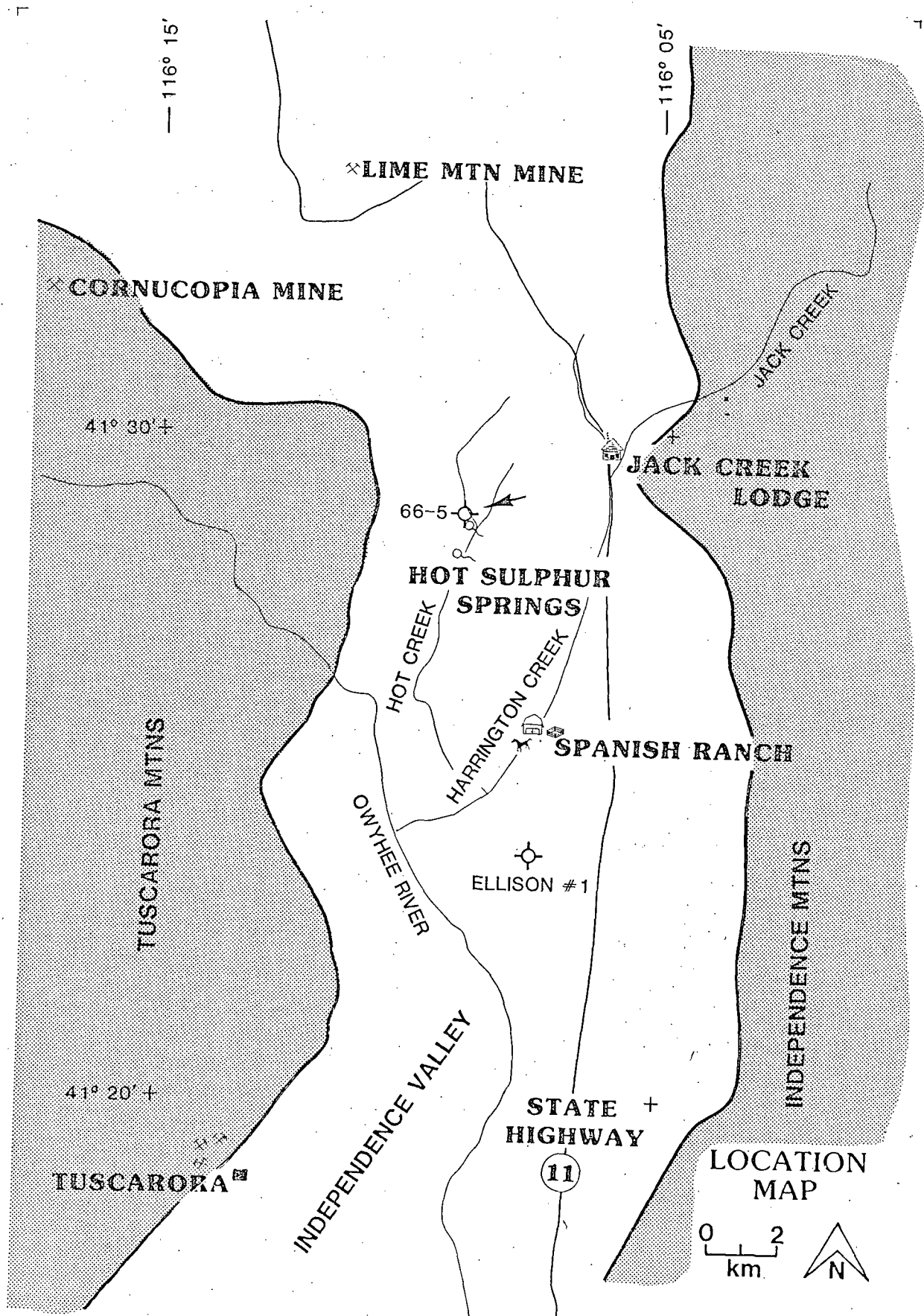


Figure 3L. Orientation map showing principal features of the Tuscarora prospect.

Figure 4L. Simplified geologic map, showing out crop of Paleozoic rocks and Tertiary volcanics Quaternary alluvium and hot spring sinter (Pilkington, 1979).



WEST — EAST GEOLOGIC CROSS-SECTION

W

E

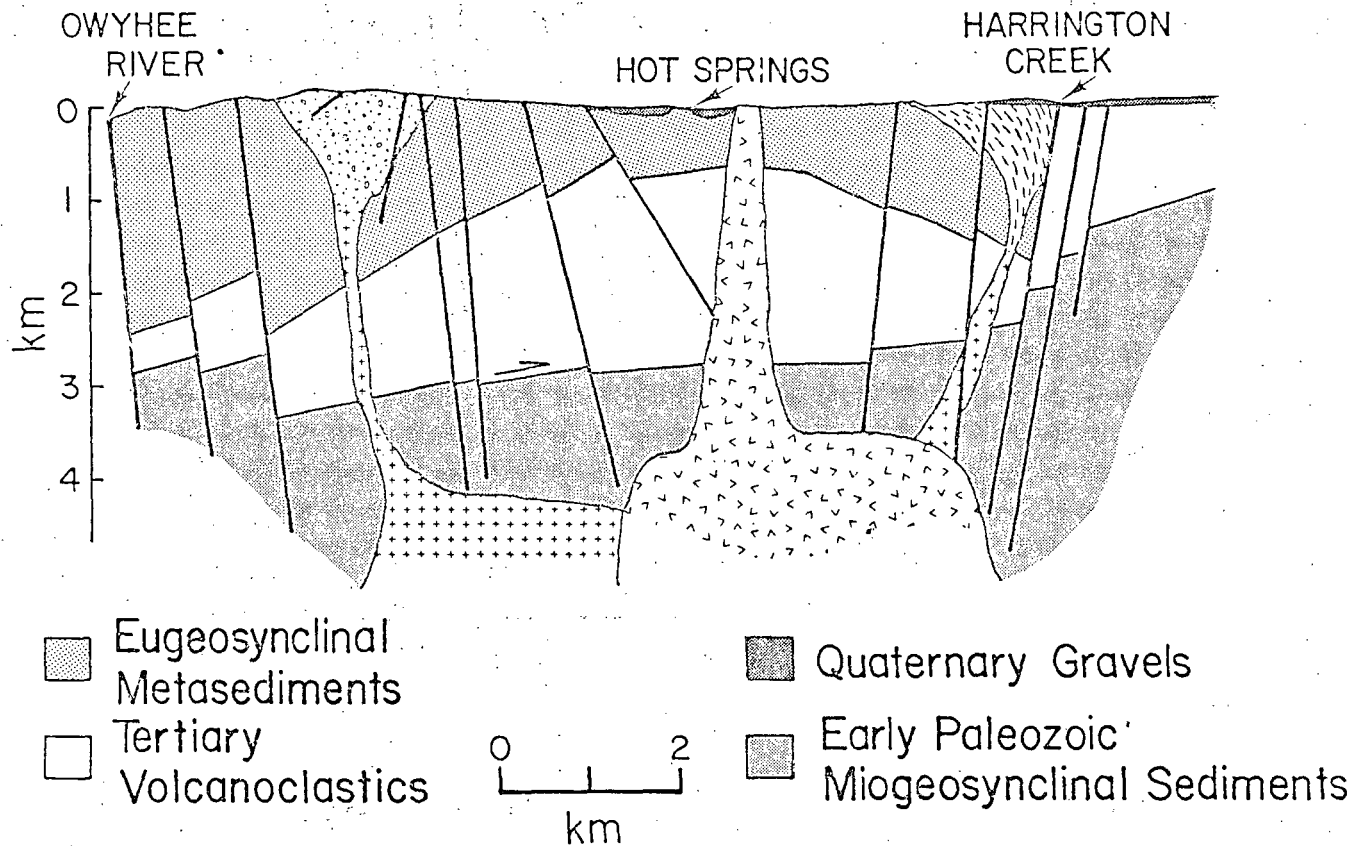


Figure 5R. East-west geologic x-section 0.5 mile south of well 66-5 (Pilkington, 1979) showing intrusions and arched paleozoic rock beneath Tertiary volcanoclastics.

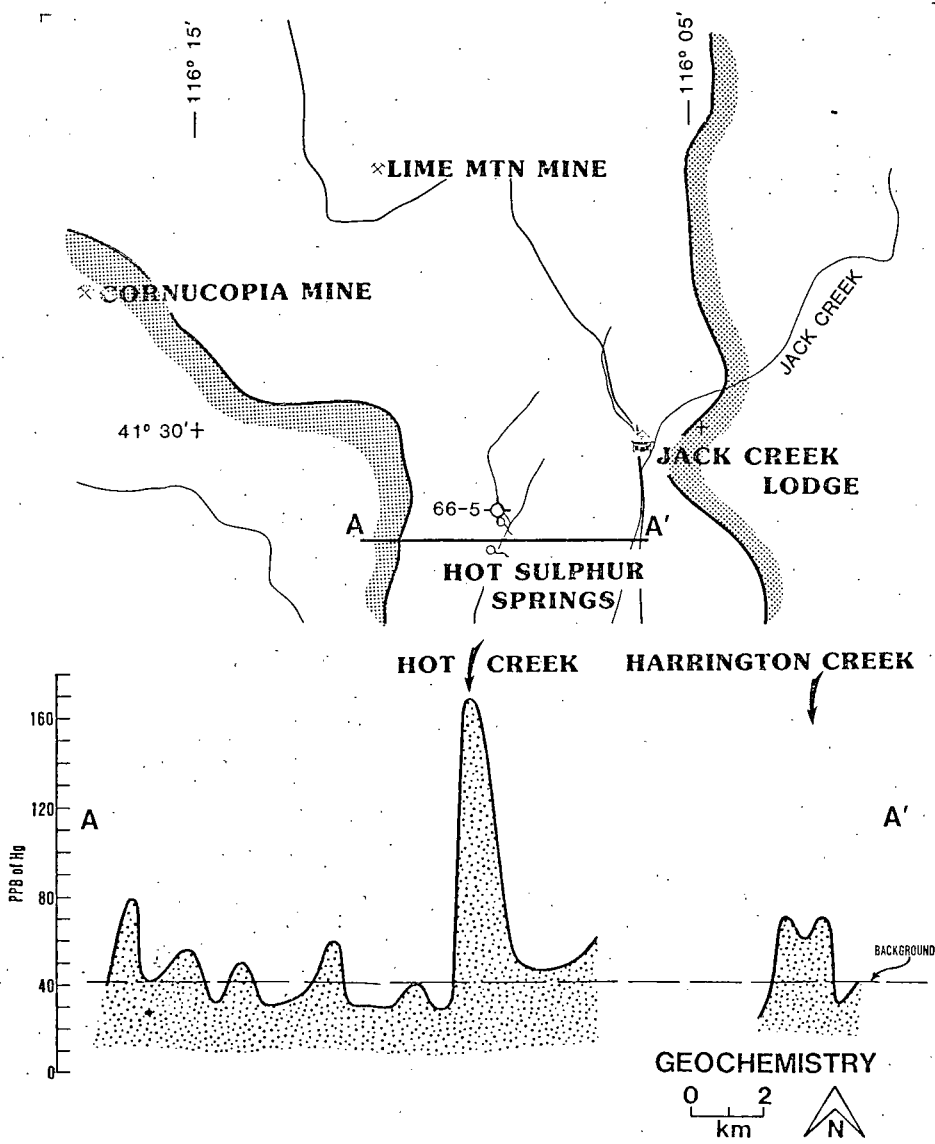


Figure 6L. Soil mercury profile and profile location.

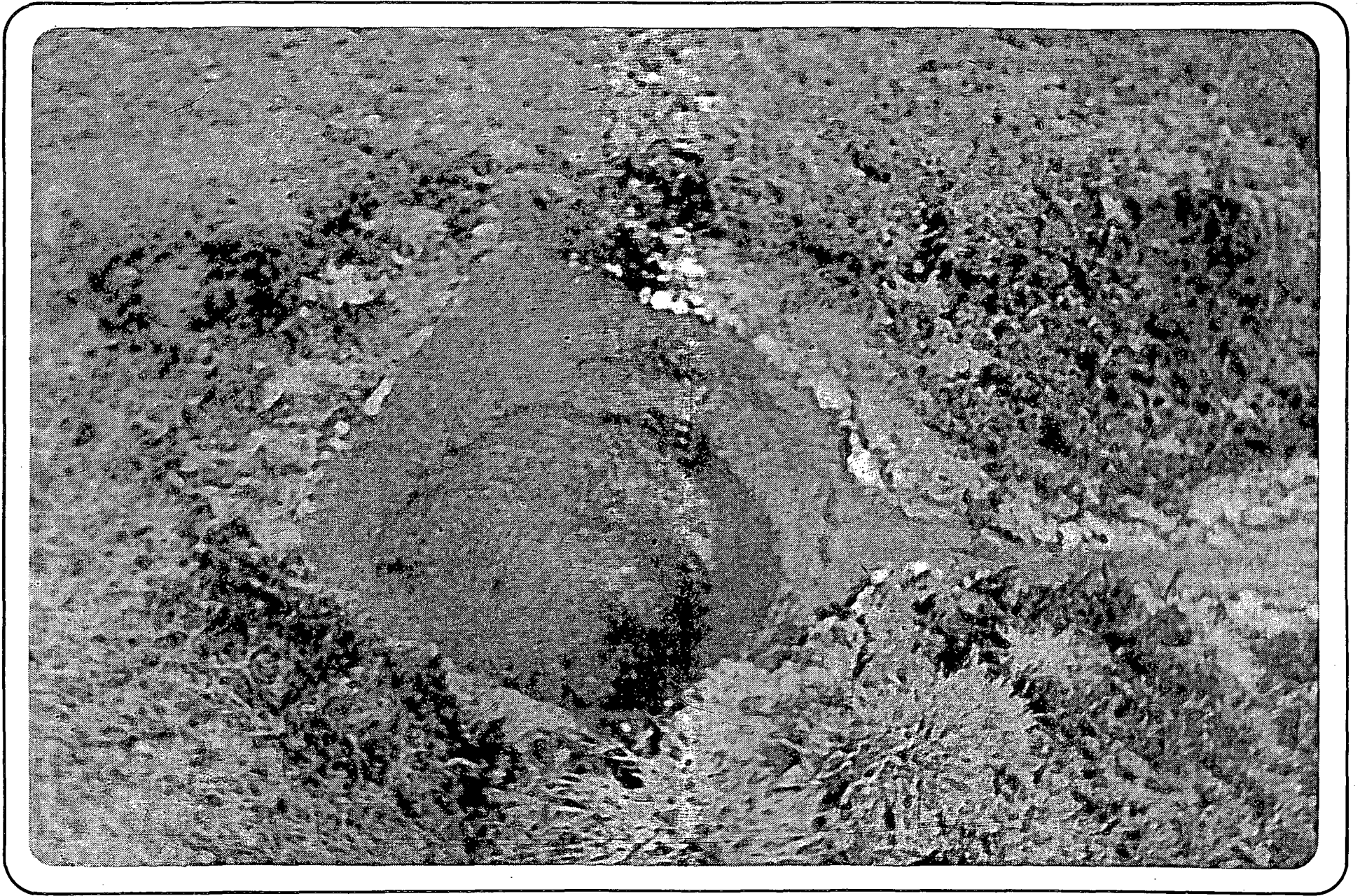


Figure 7R. View of small hot pool in the lower hot springs group.

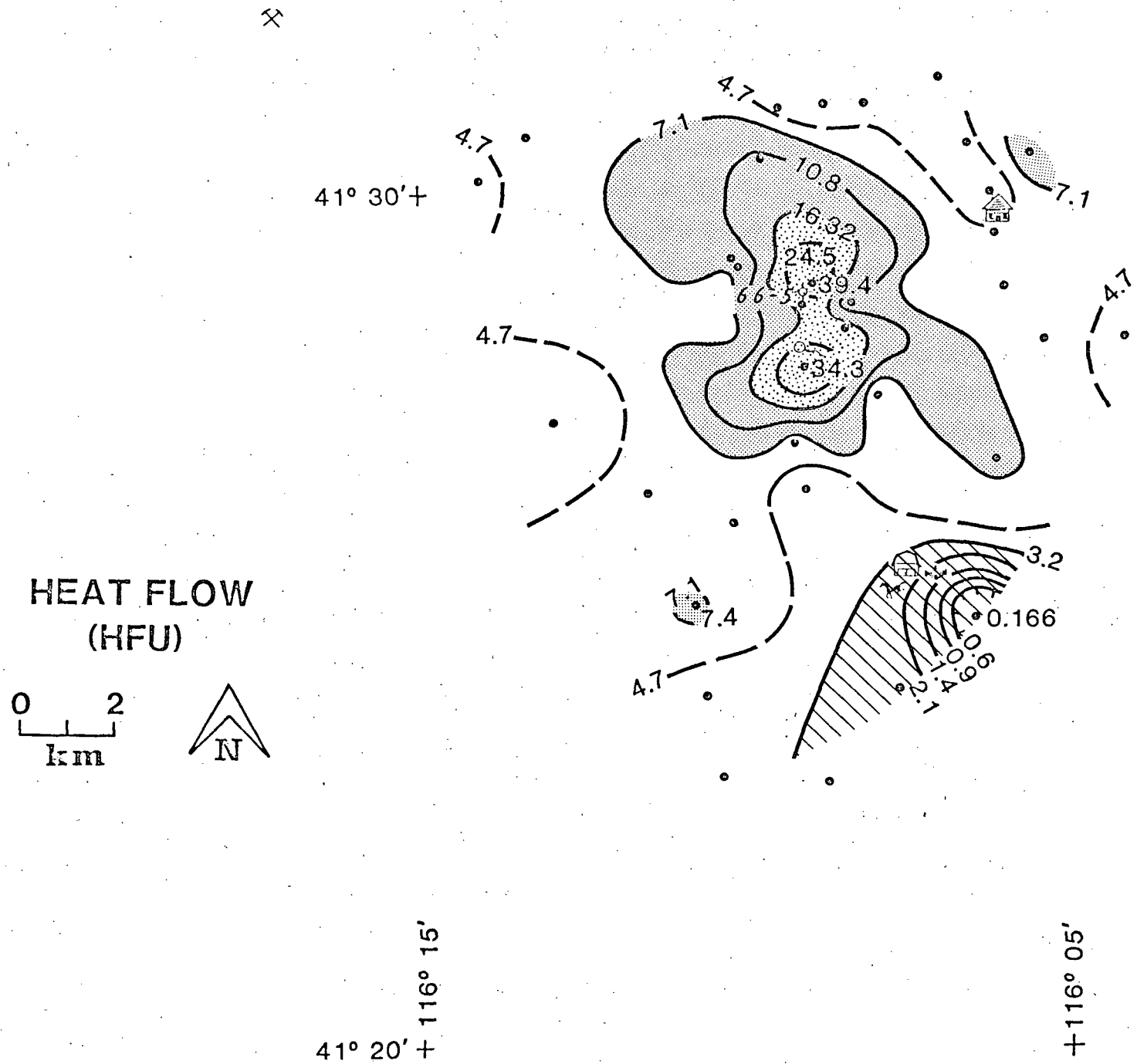


Figure 8L. Heatflow map showing profile locations.

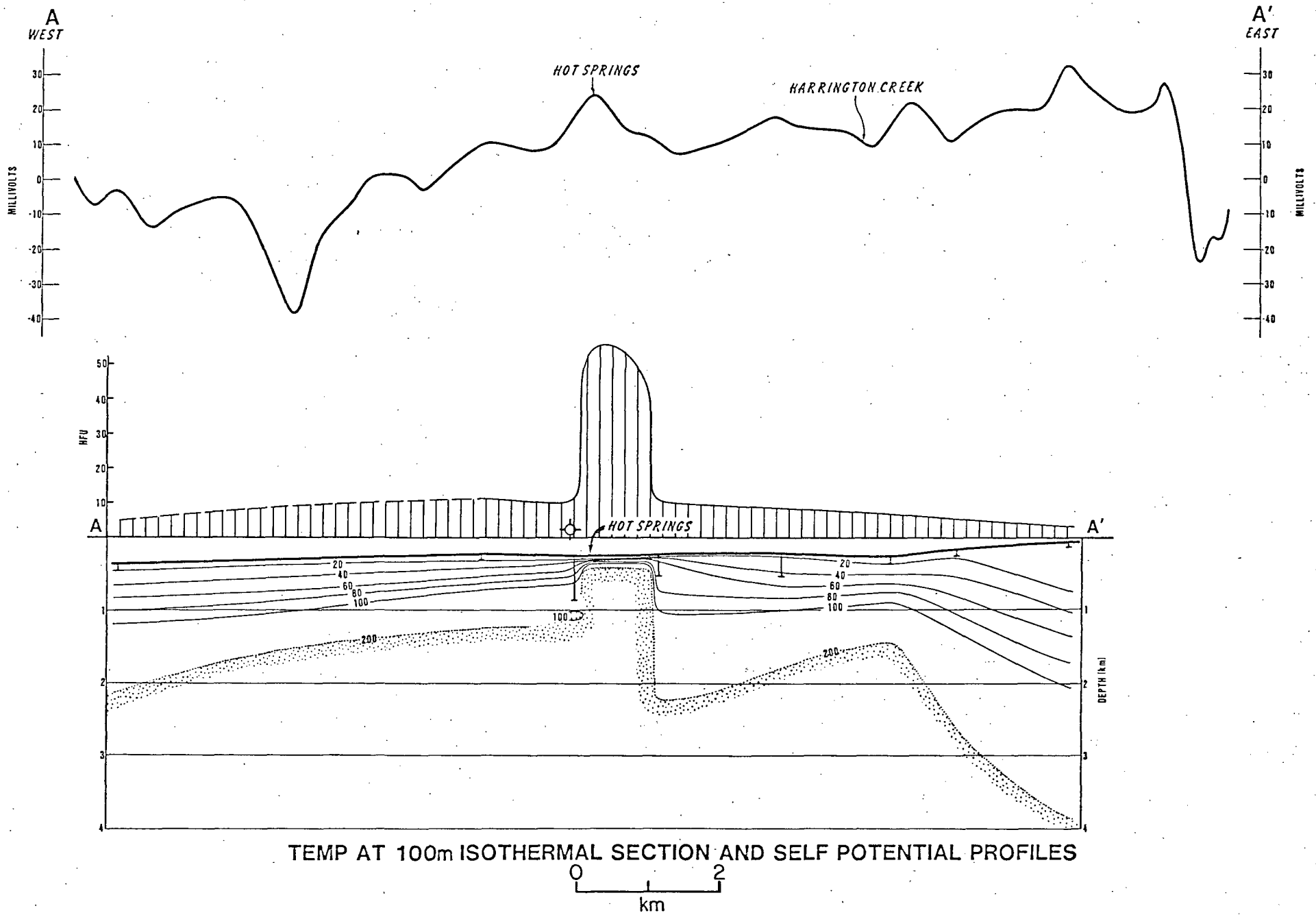
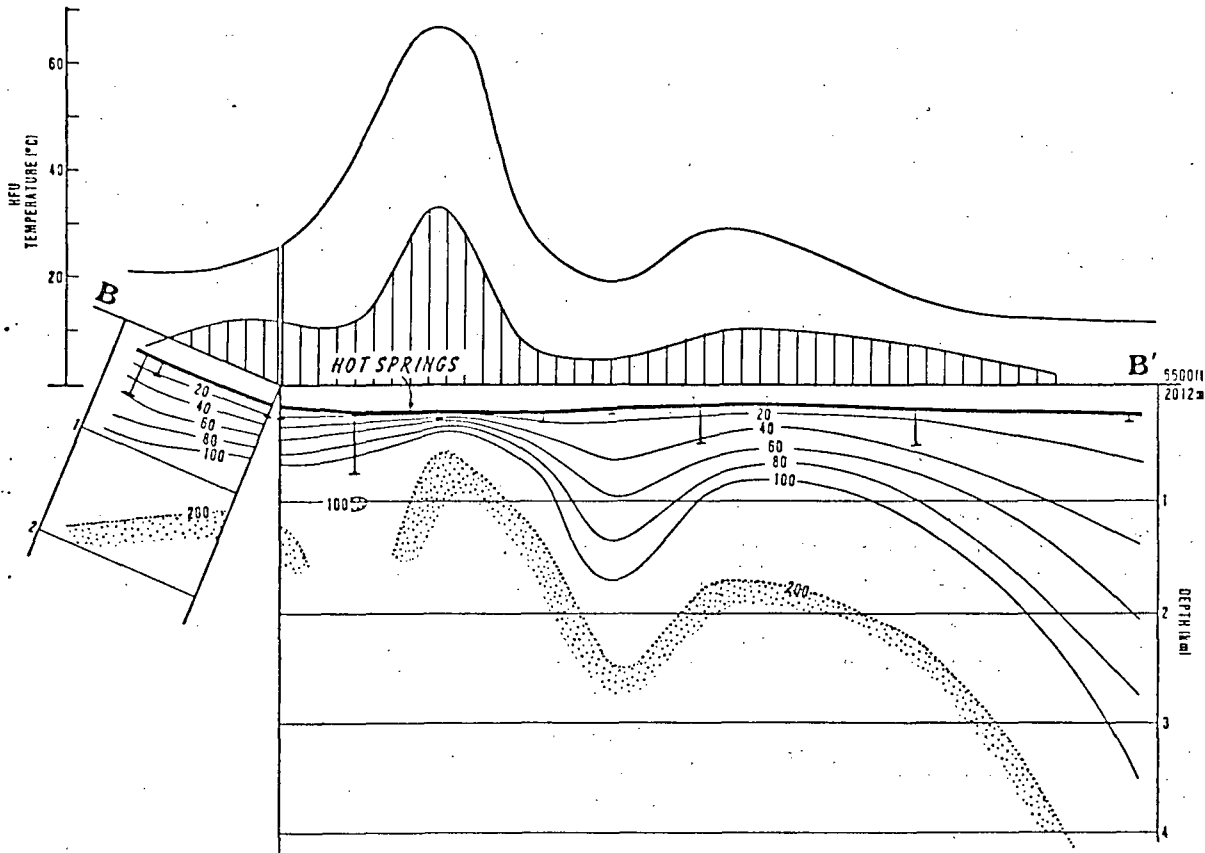
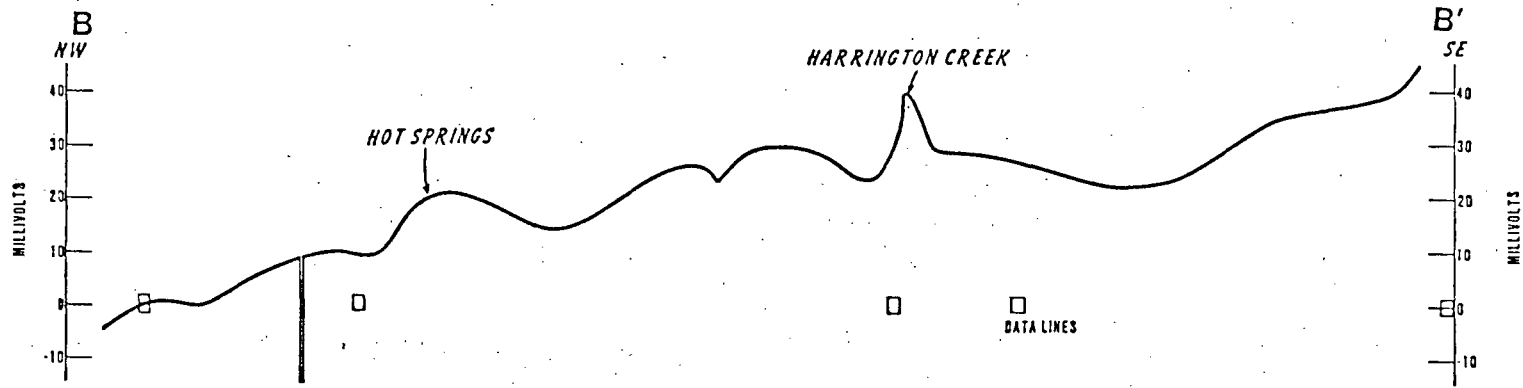
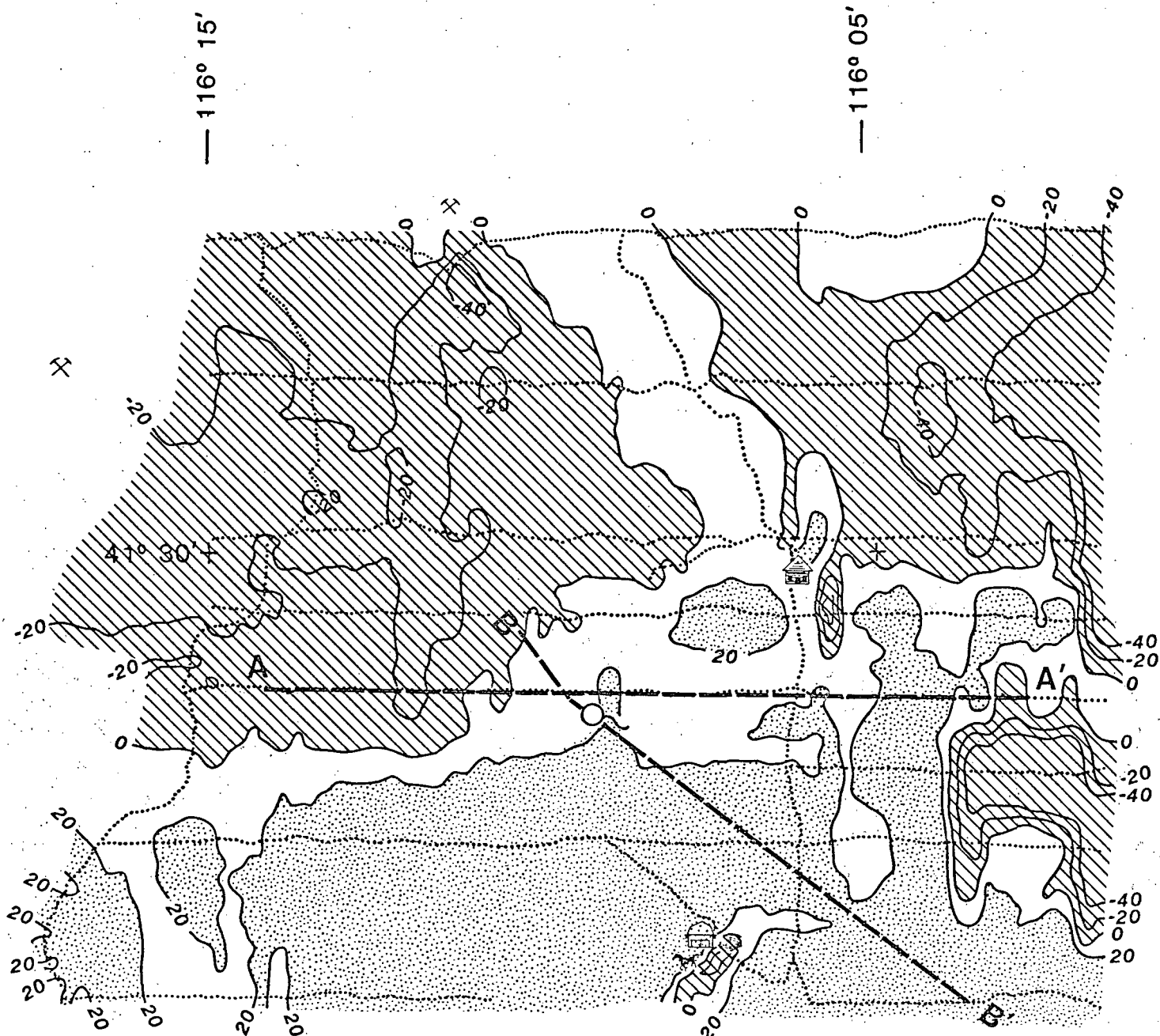


Figure 9R. East-west heatflow profile A-A' showing isotherms and SP anomaly.

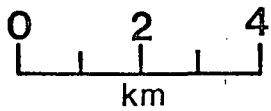


TEMP AT 100m ISOTHERMAL SECTION AND SELF POTENTIAL PROFILES

Figure 10R. Northwest-southeast heatflow profile B-B' showing temperature at 100 meters (curve just above isotherms) isotherms and SP anomaly.



SELF POTENTIAL IN MILLIVOLTS



$41^{\circ} 20' +$

Figure 11L. Self-potential map showing profile locations.

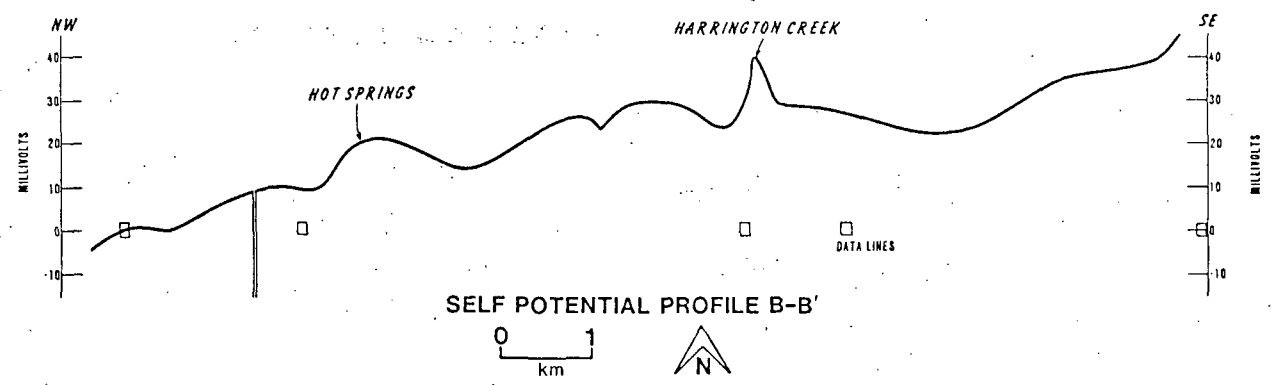
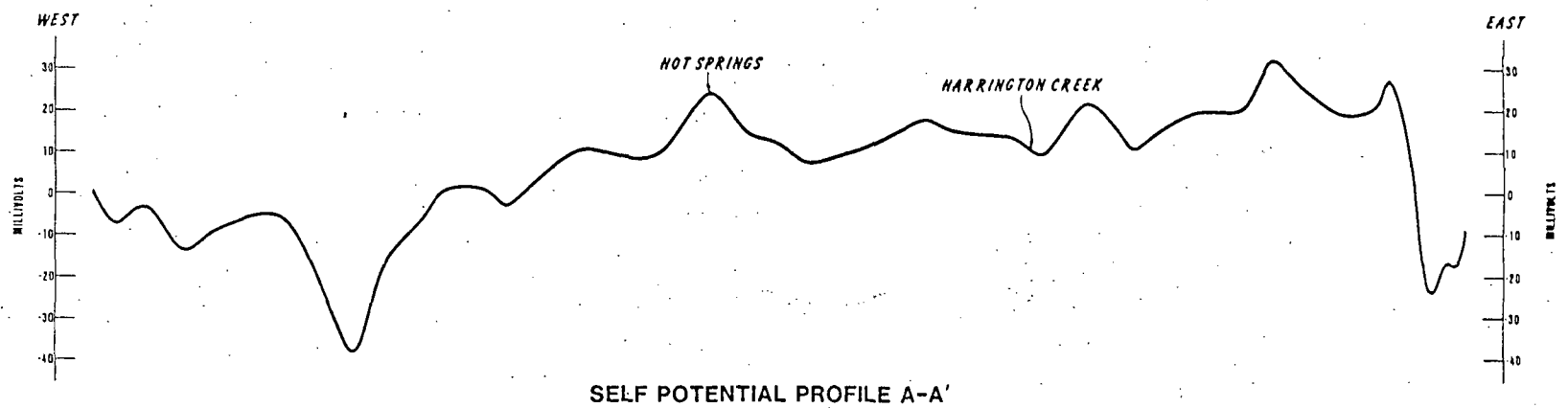
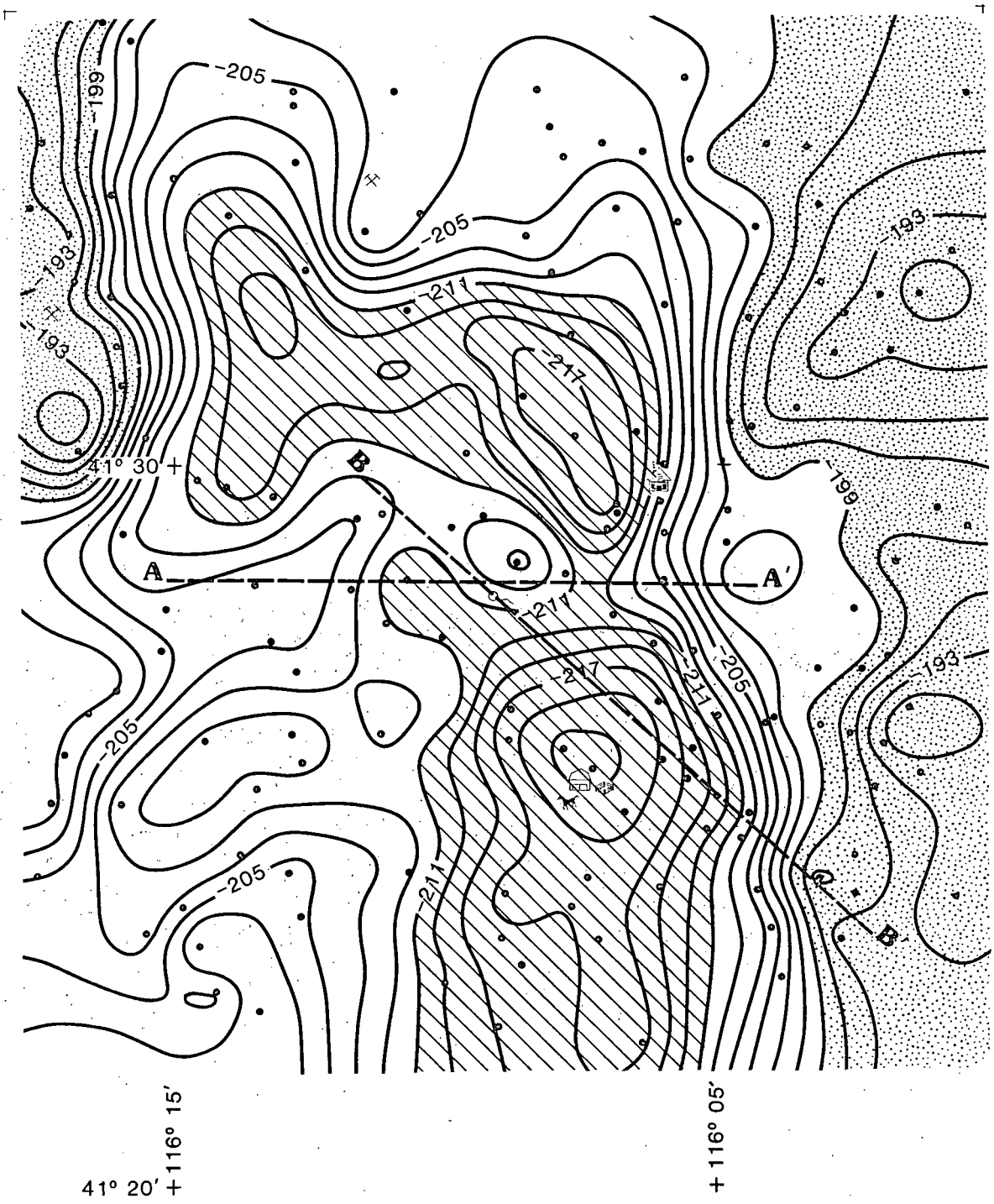


Figure 12R. Self-potential profiles A-A' and B-B'.



**COMPLETE BOUGUER
ANOMALY GRAVITY MAP**

• GRAVITY STATIONS

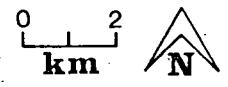
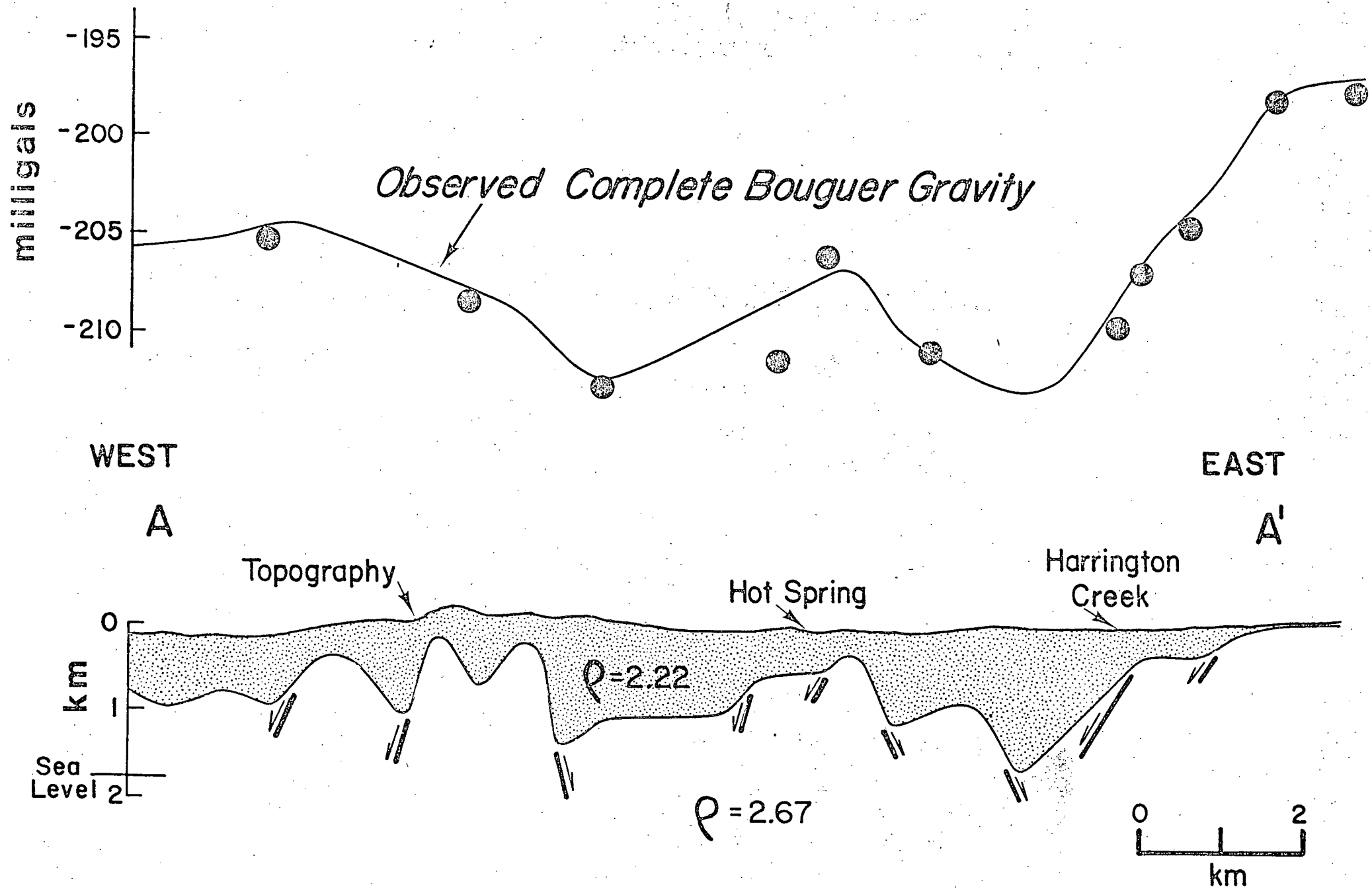
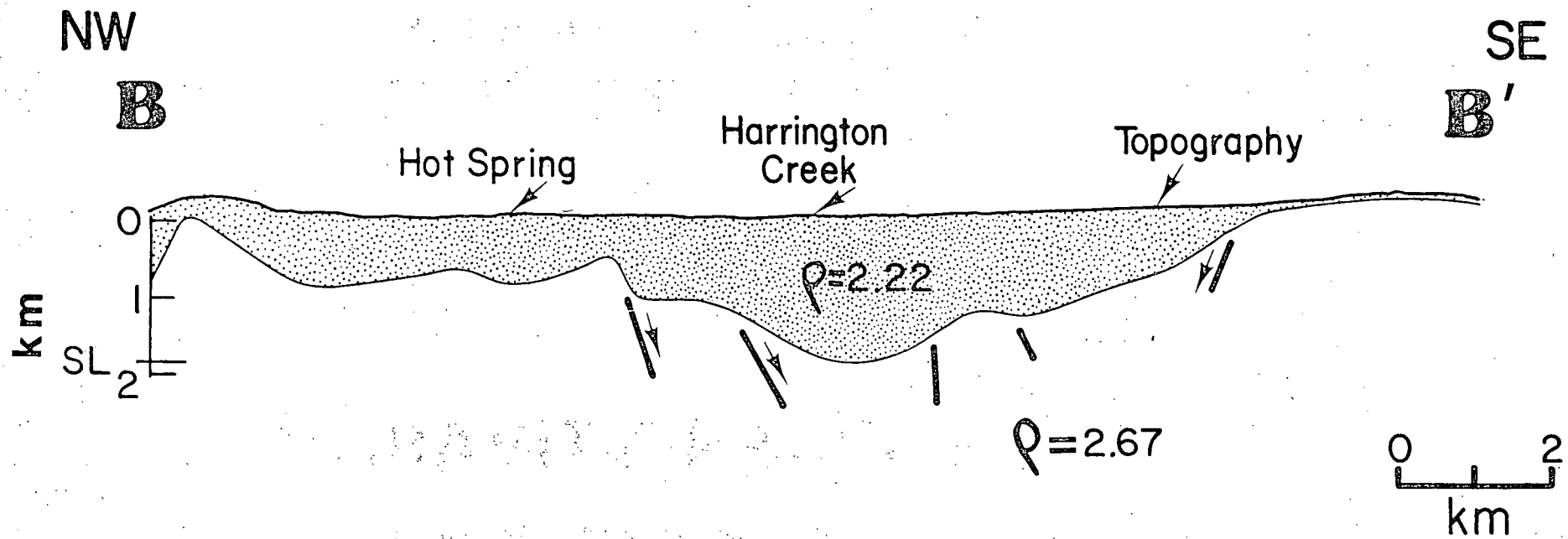
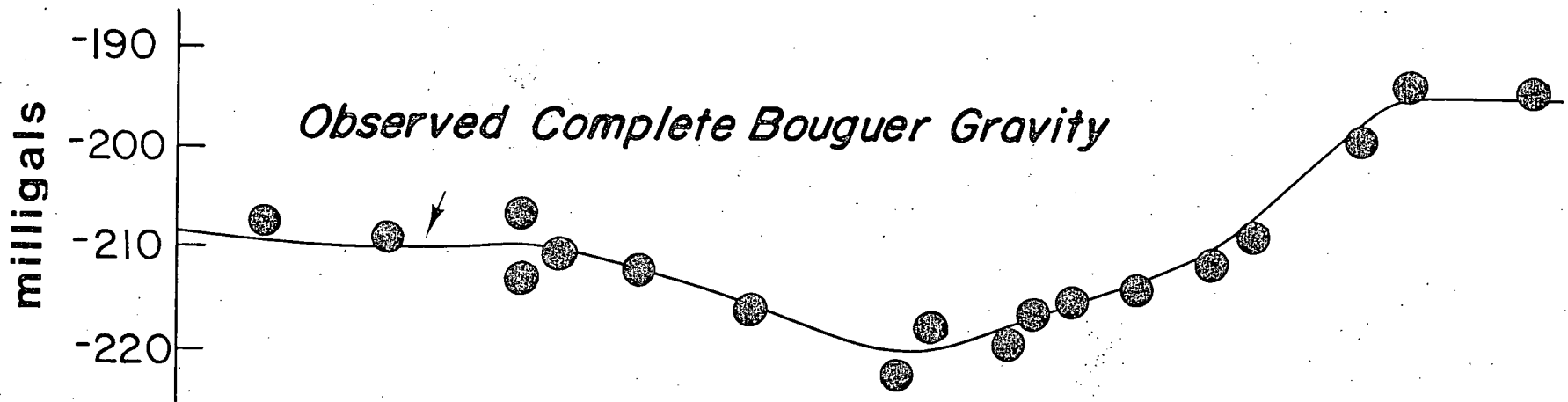


Figure 13L. Complete Bouguer gravity map.



GRAVITY PROFILE A-A'

Figure 14R. East-west gravity profile A-A' and depth section.



GRAVITY PROFILE B-B'

Figure 15R. Northwest-southeast profile B-B' and depth section.

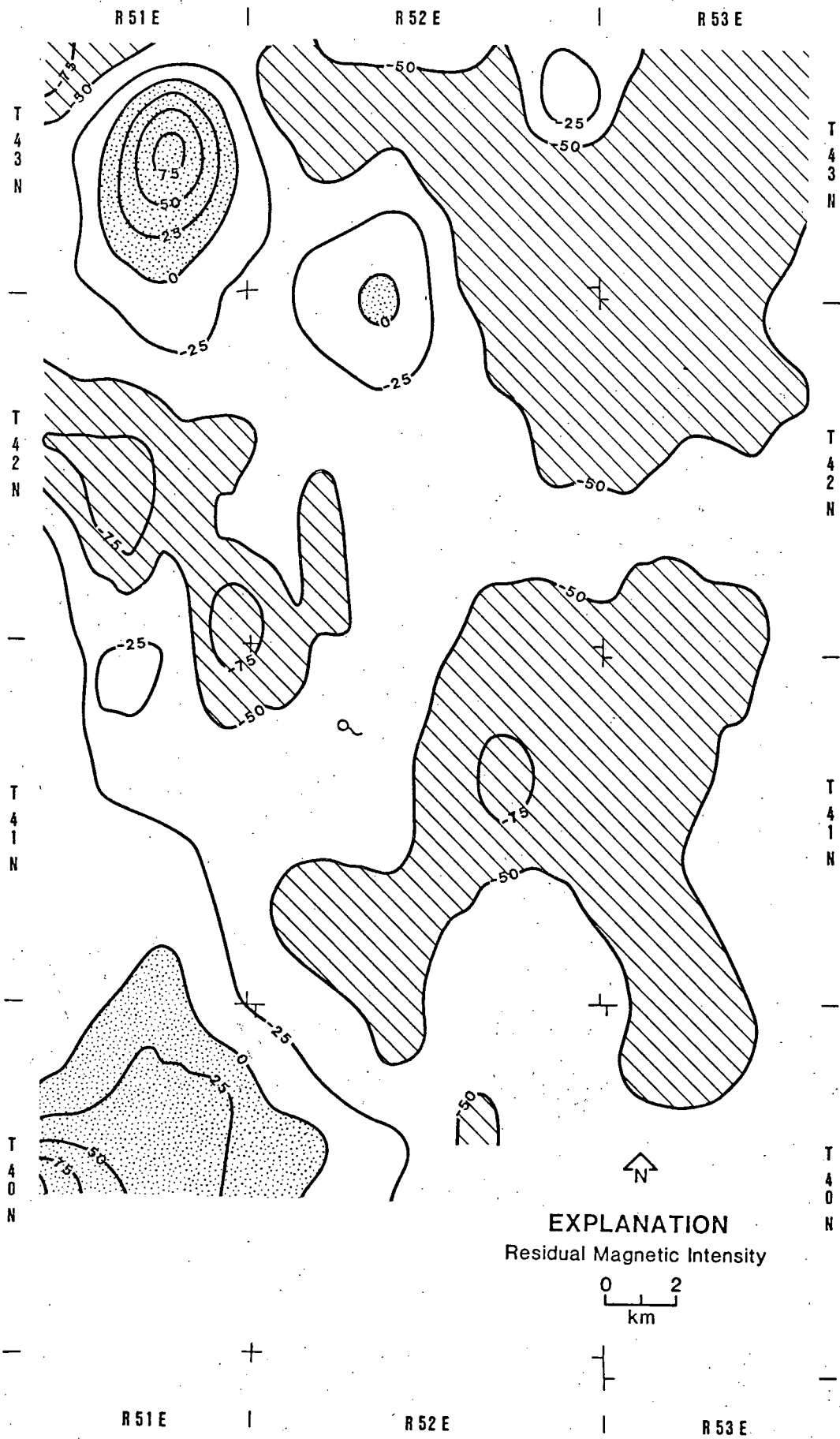


Figure 16L. Residual magnetic map.

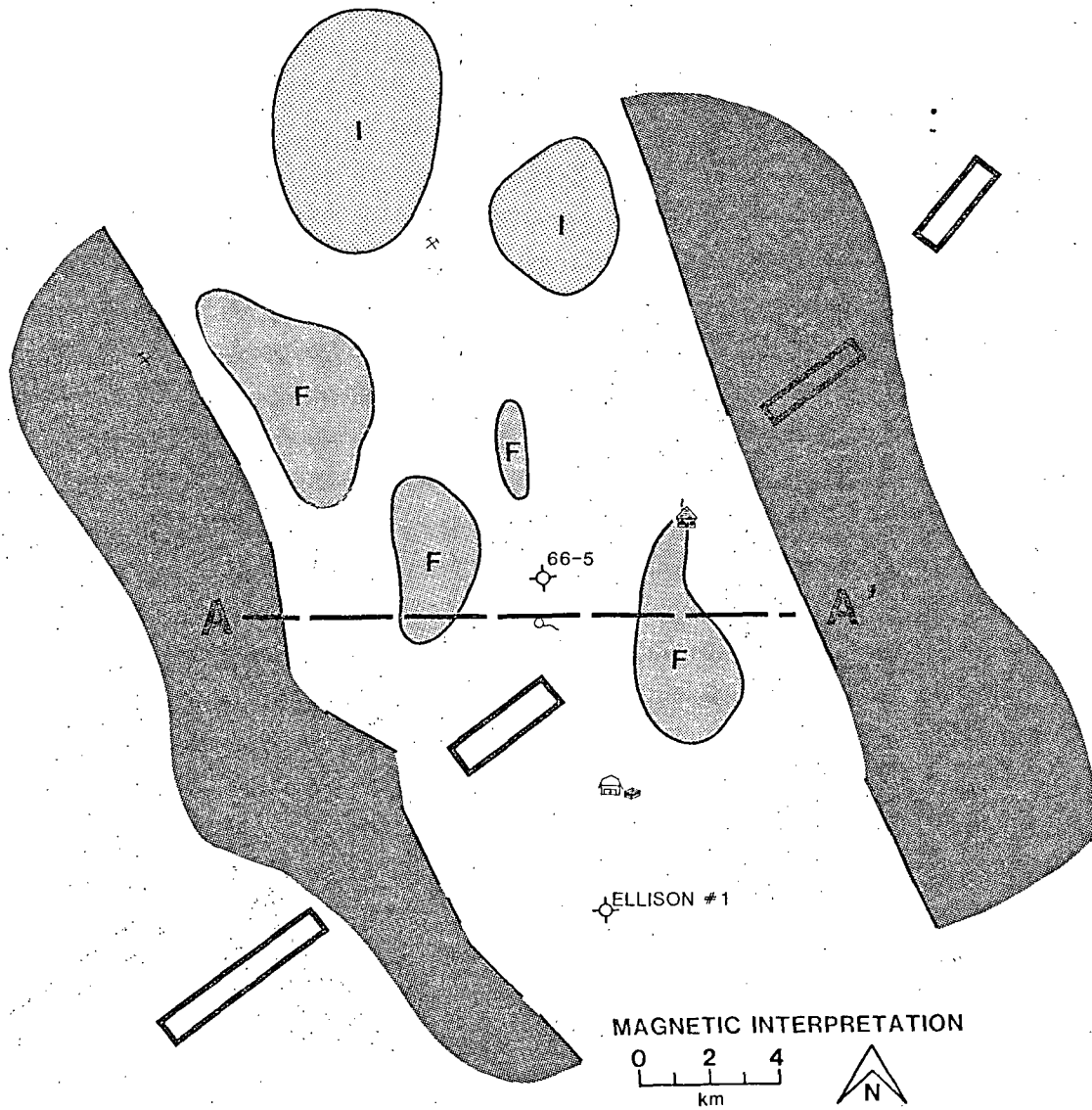


Figure 17R. Magnetic interpretation and profile A-A' location.

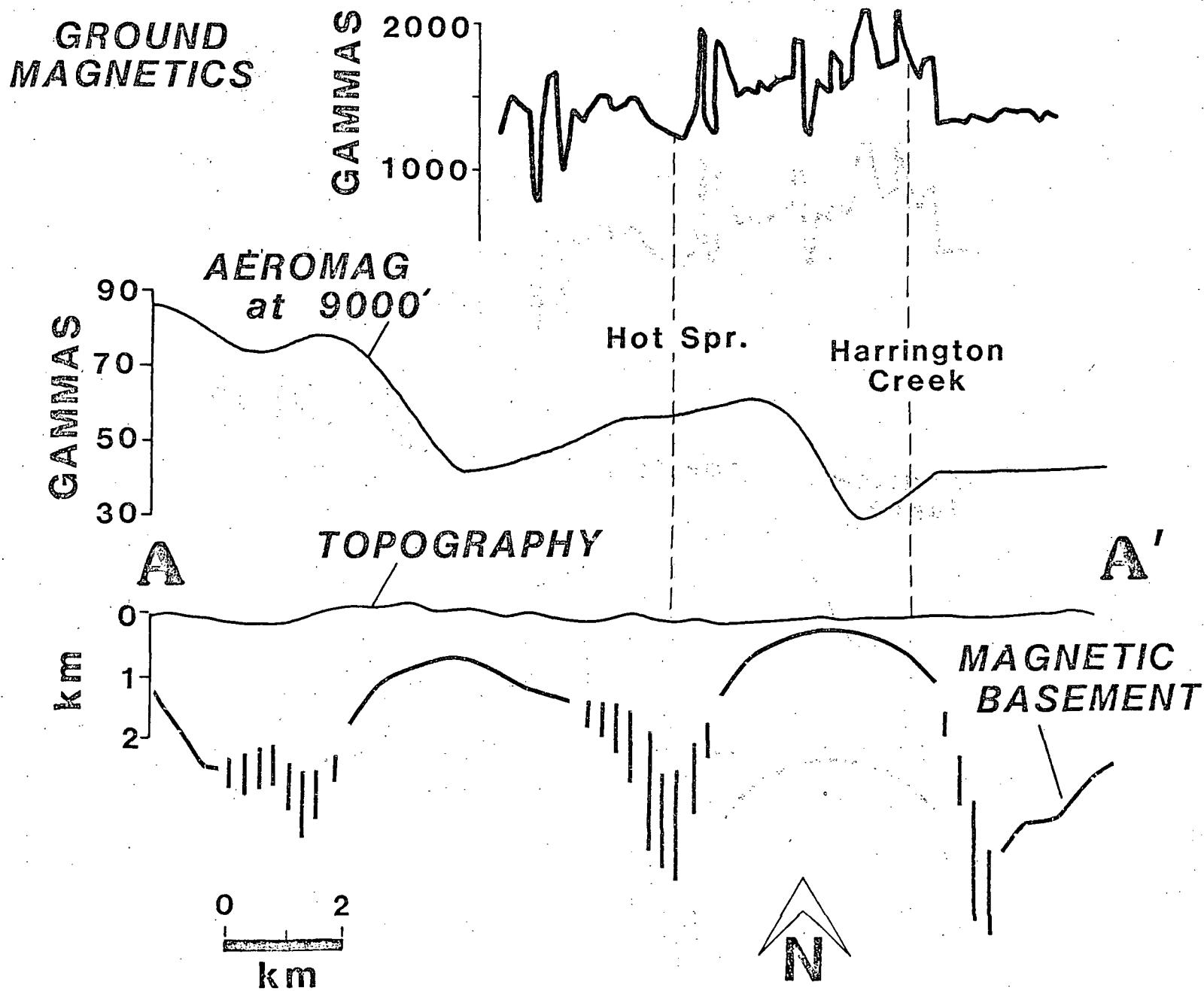
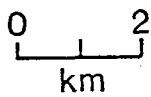


Figure 17Ra. Magnetic profile A-A' showing ground magnetics, aeromagnetics and depth to magnetic basement.

T
4
2
N



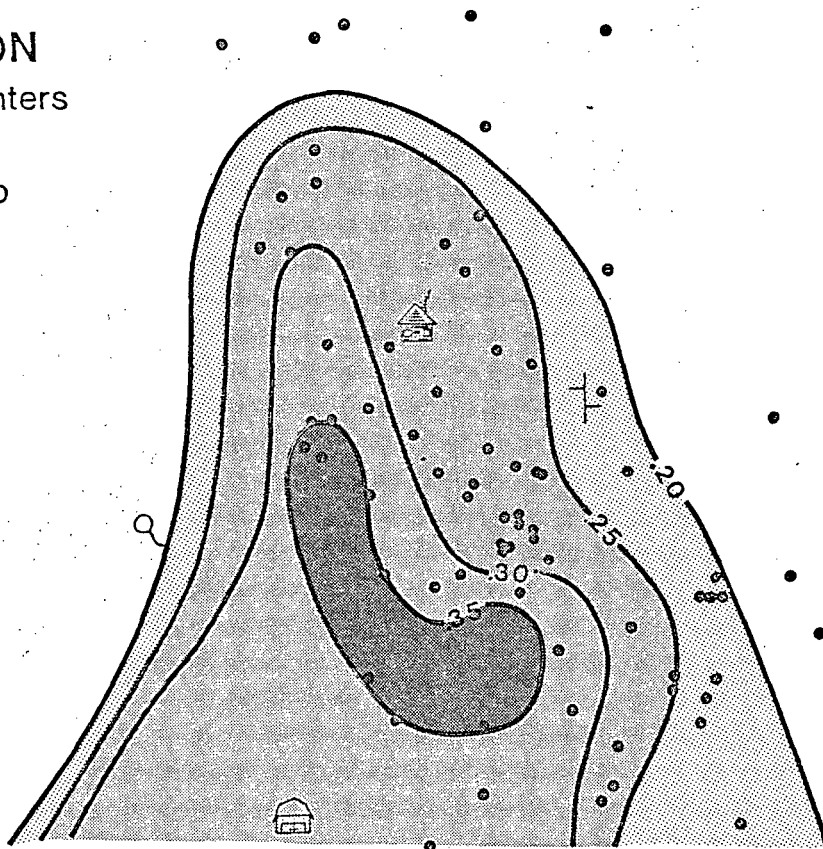
EXPLANATION
Earthquake Epicenters
and
Poisson's Ratio



—

+

T
4
1
N



—

+

+

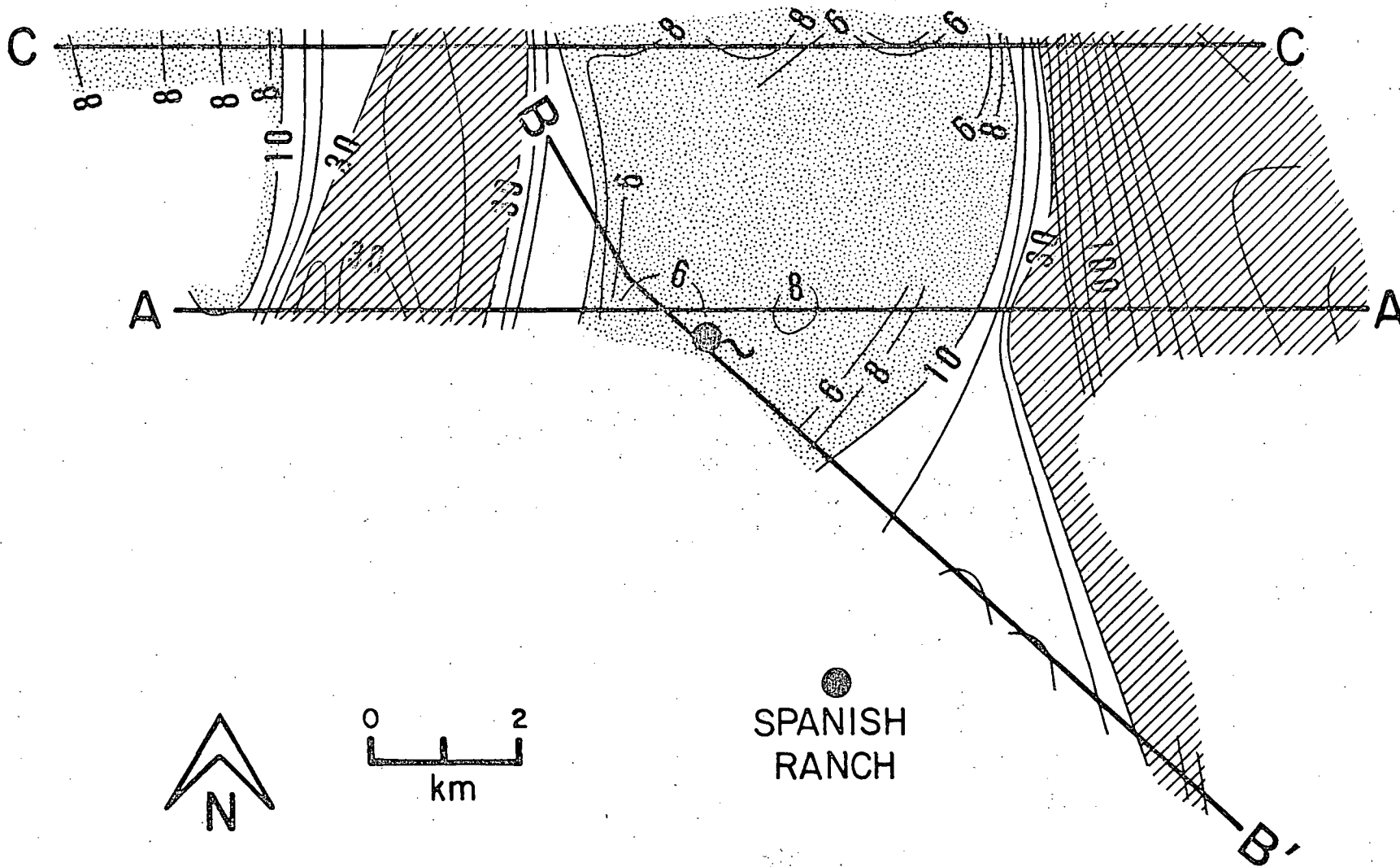
R 51 E

|

R 52 E

|

Figure 18L. Map of Poisson's Ratio and earthquake epicenters.



DIPOLE-DIPOLE RESISTIVITY

N=2 A=610m

Figure 19L. Dipole-dipole resistivity for N=2 and A=610 meters showing profile locations.

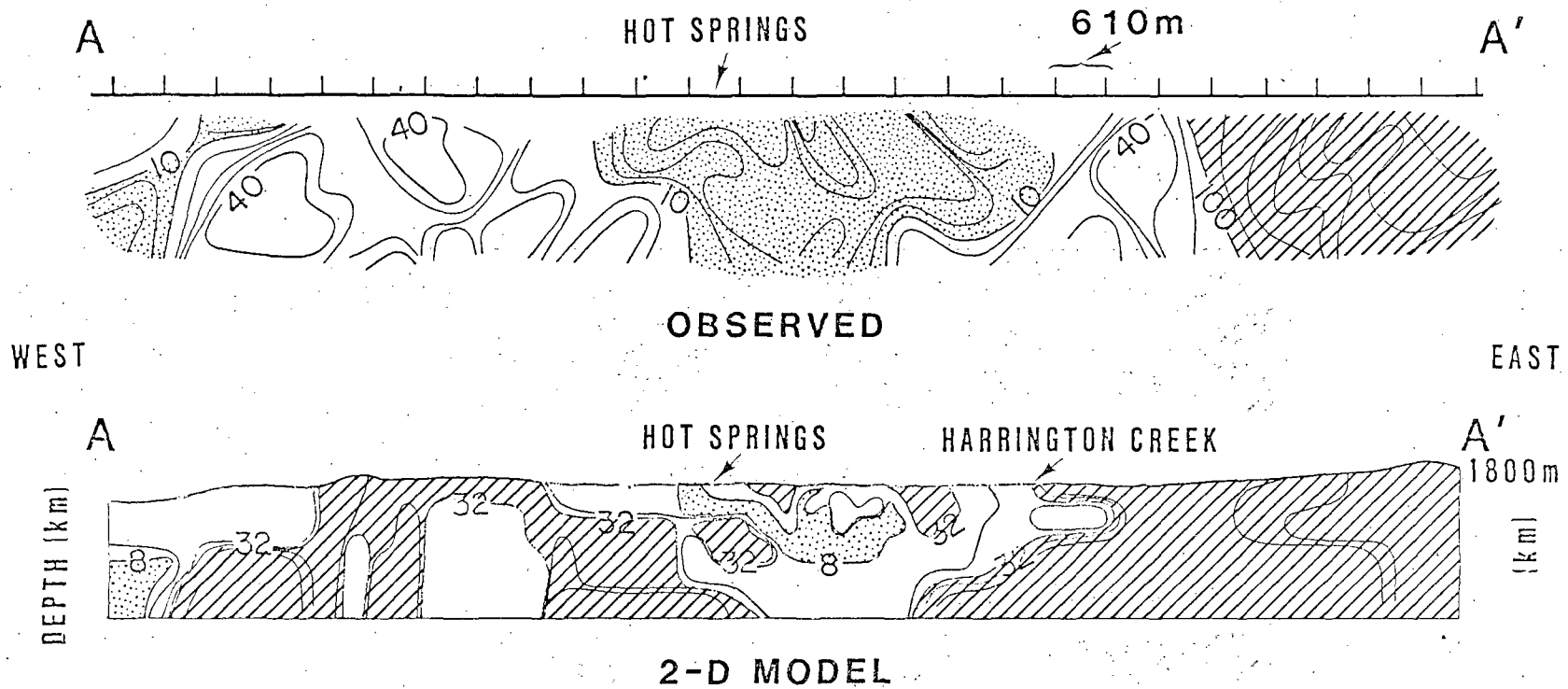
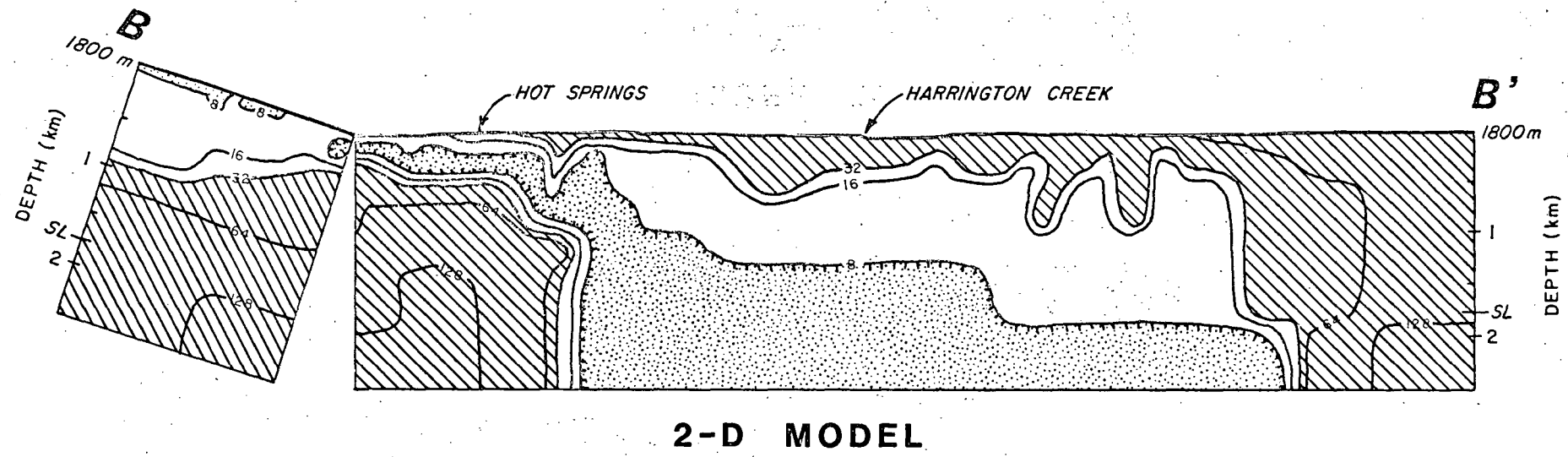
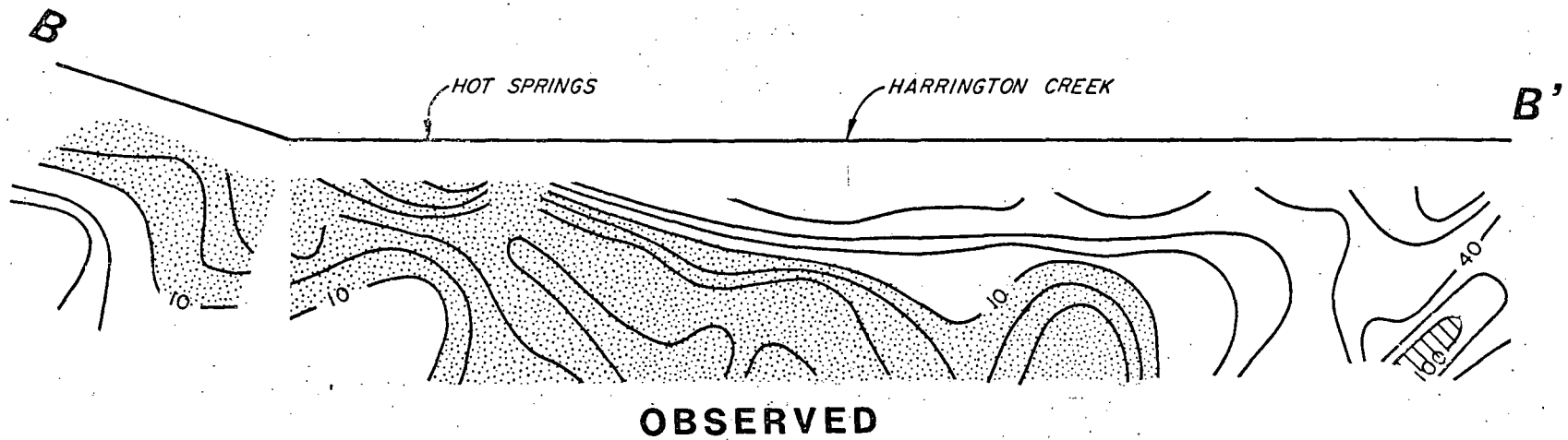


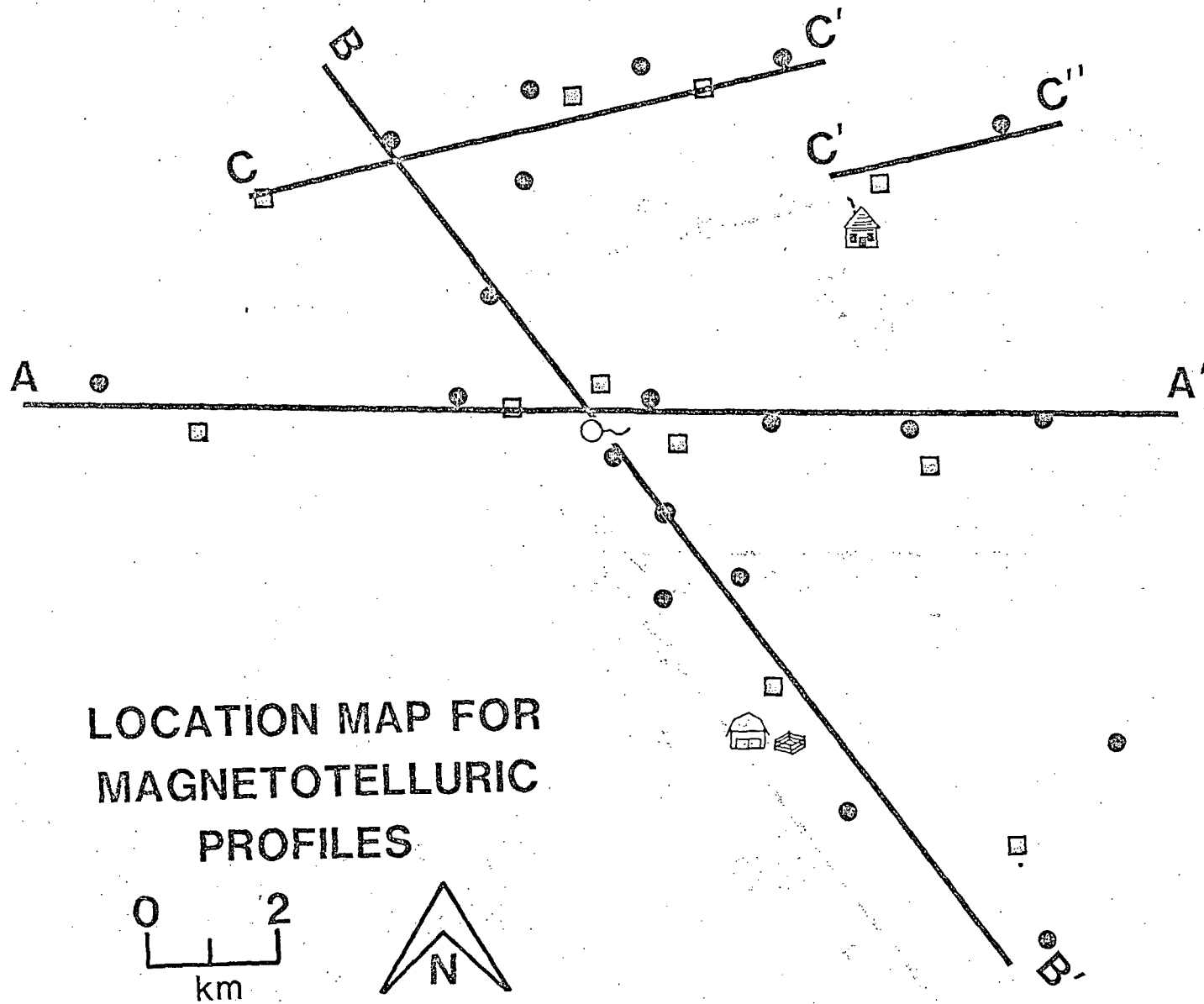
Figure 20R. Resistivity section A-A' showing observed apparent resistivity pseudosection and modelled resistivity section.



DIPOLE - DIPOLE RESISTIVITY



Figure 21R. Resistivity section B-B' showing observed apparent resistivity pseudosection and modelled resistivity depth section.



**LOCATION MAP FOR
MAGNETOTELLURIC
PROFILES**

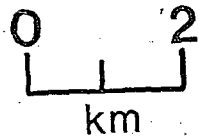
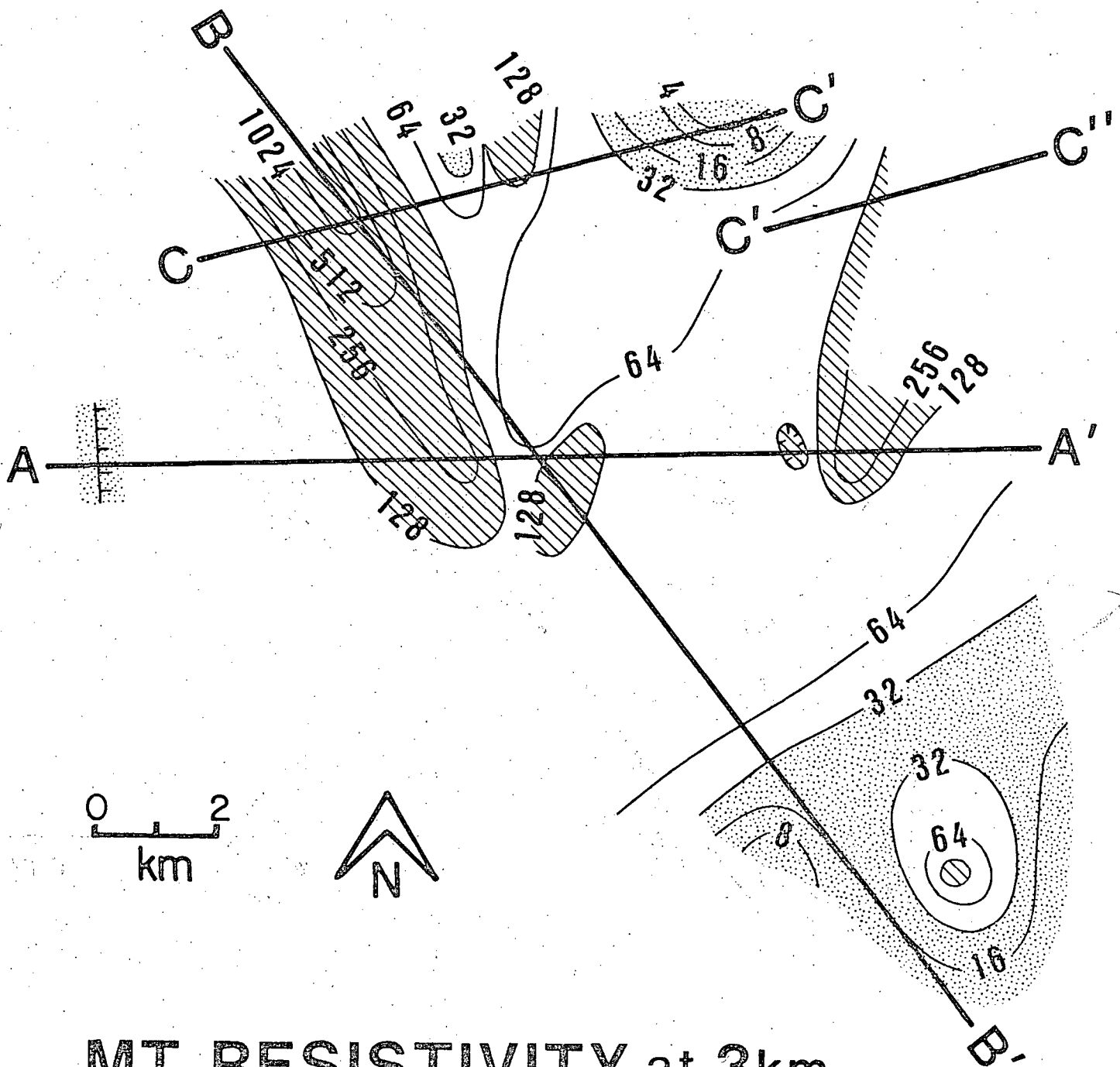
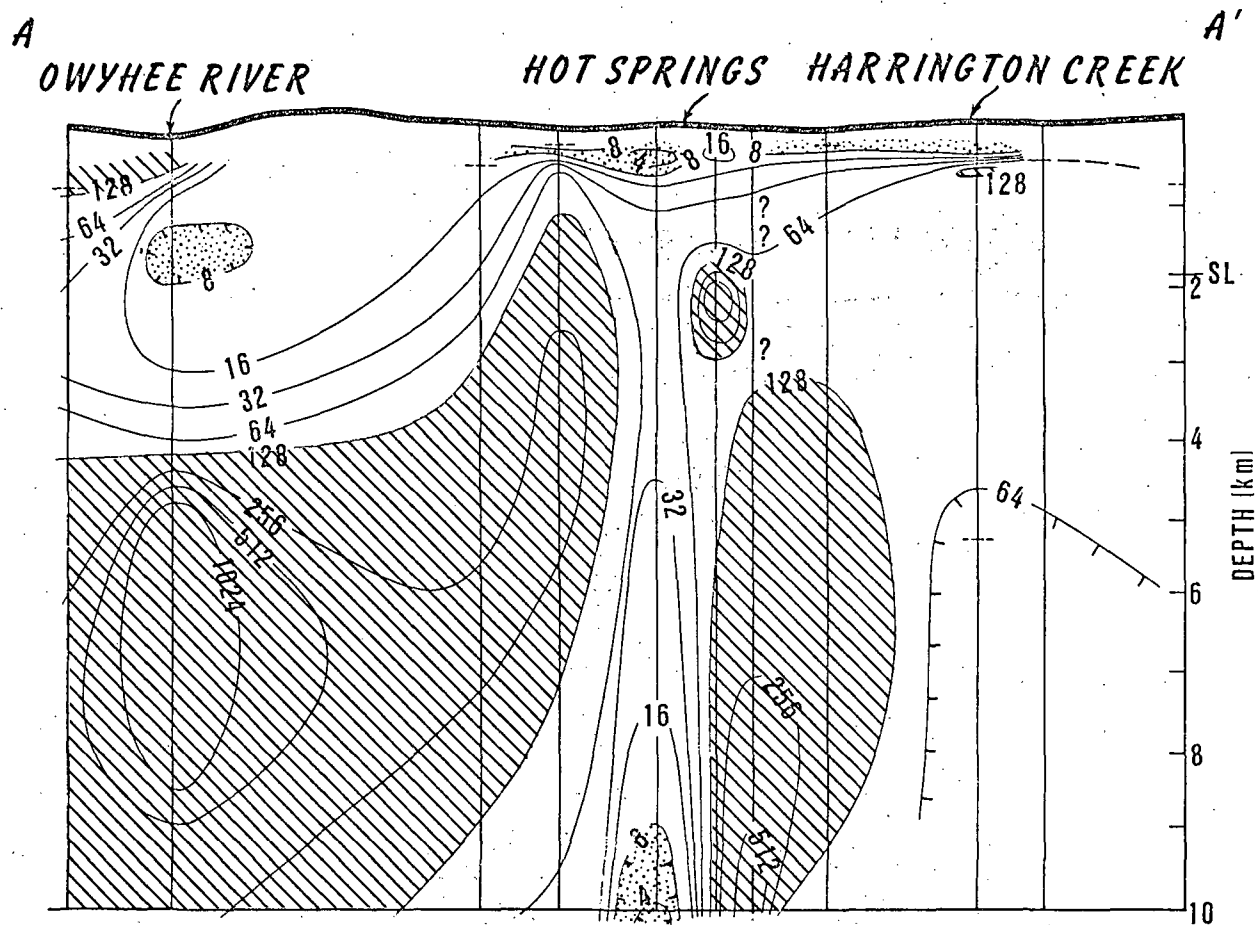


Figure 22L. Magnetotelluric stations and profile location map.



MT RESISTIVITY at 3km

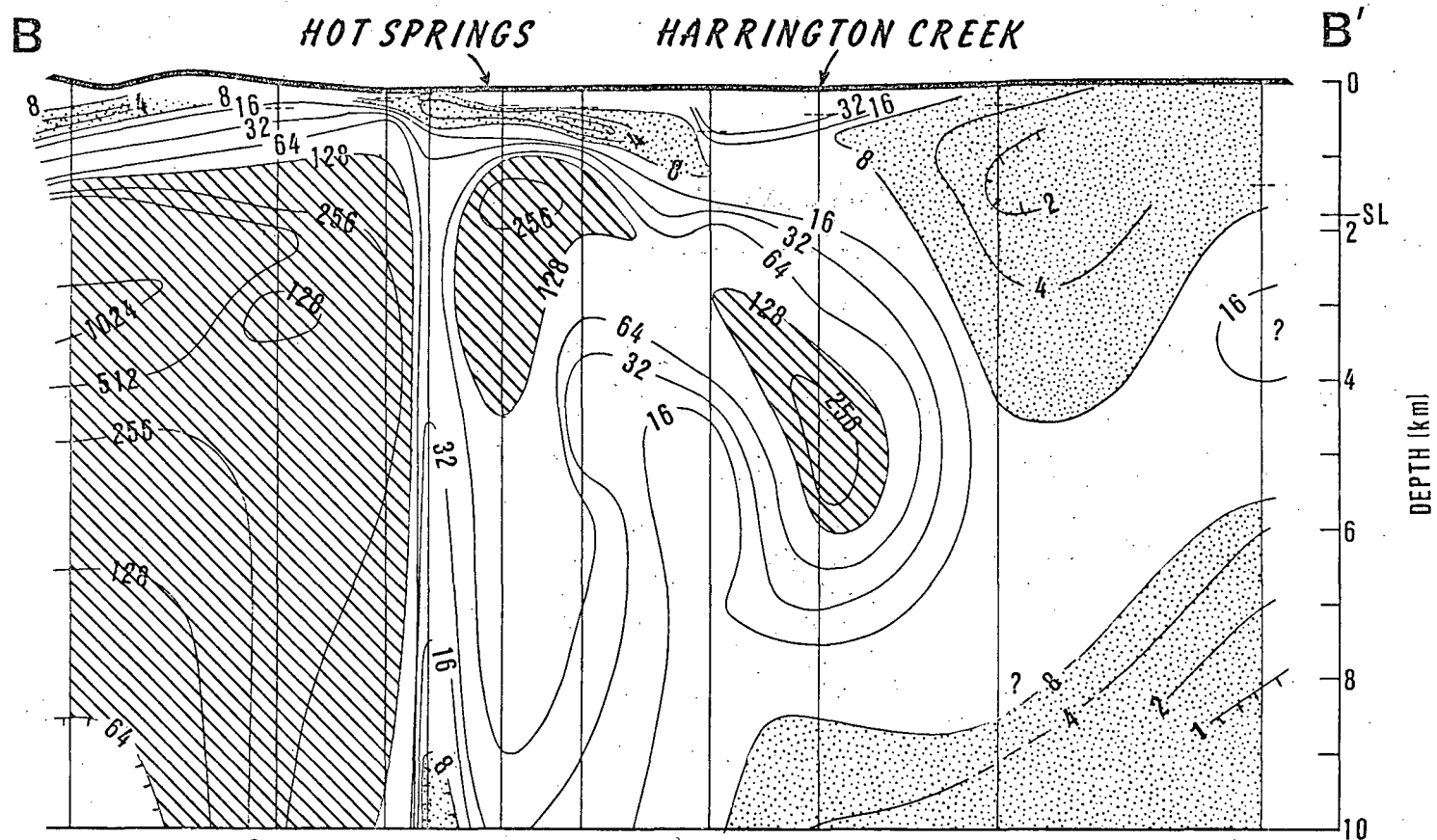
Figure 23L. Resistivity at 3km from 1-D magnetotelluric inversion.



MAGNETOTELLURIC T_e MODE 1-D INVERSION A-A'

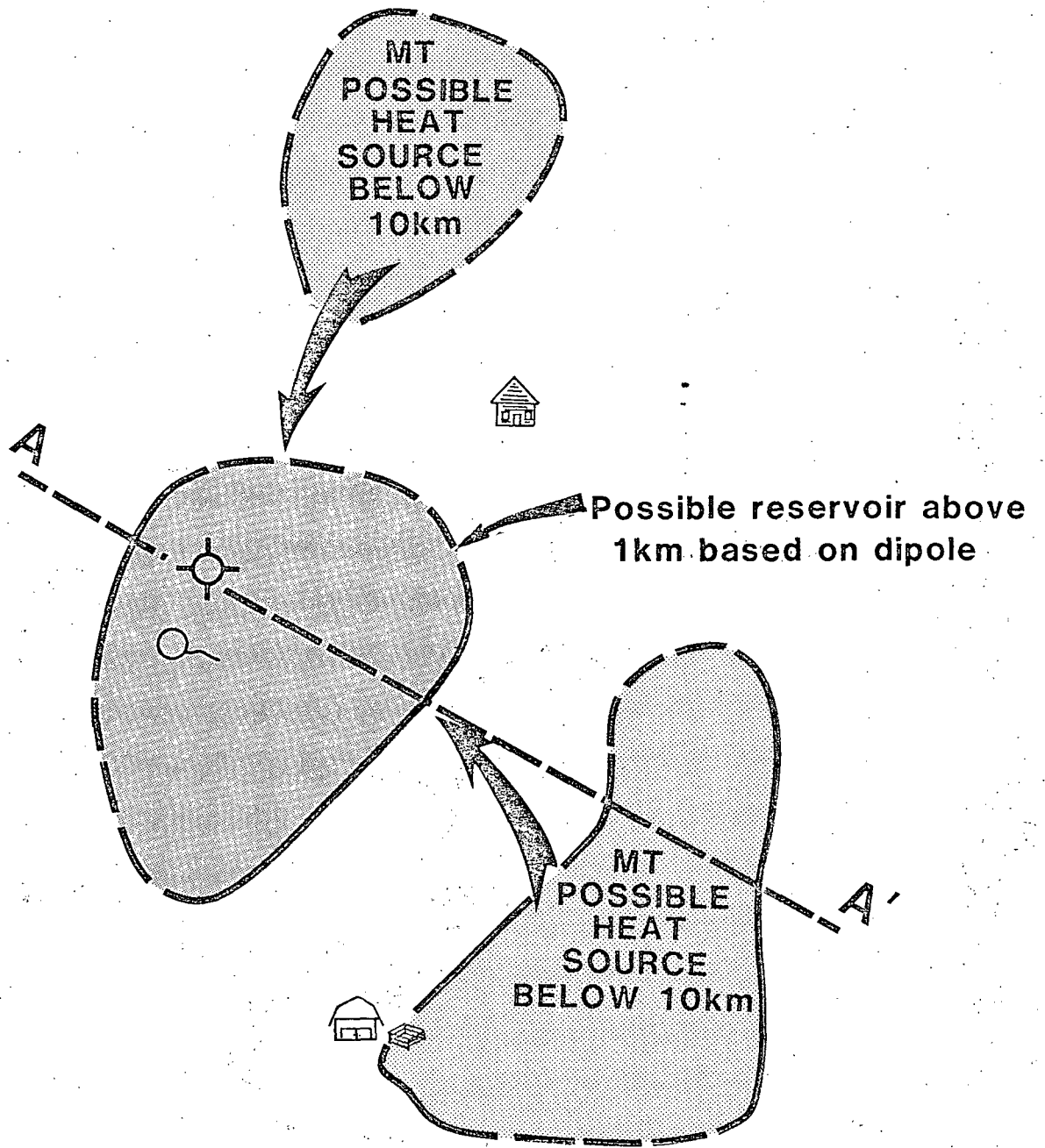
0 2
km

Figure 24R. MT resistivity section (T_e mode) along profile A-A'.



MAGNETOTELLURIC T_e MODE 1-D INVERSION B-B'

Figure 25R. MT resistivity section (T_e mode) along profile B-B'.



RESERVOIR CONCEPT

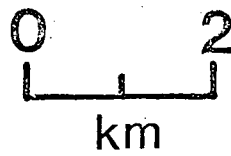
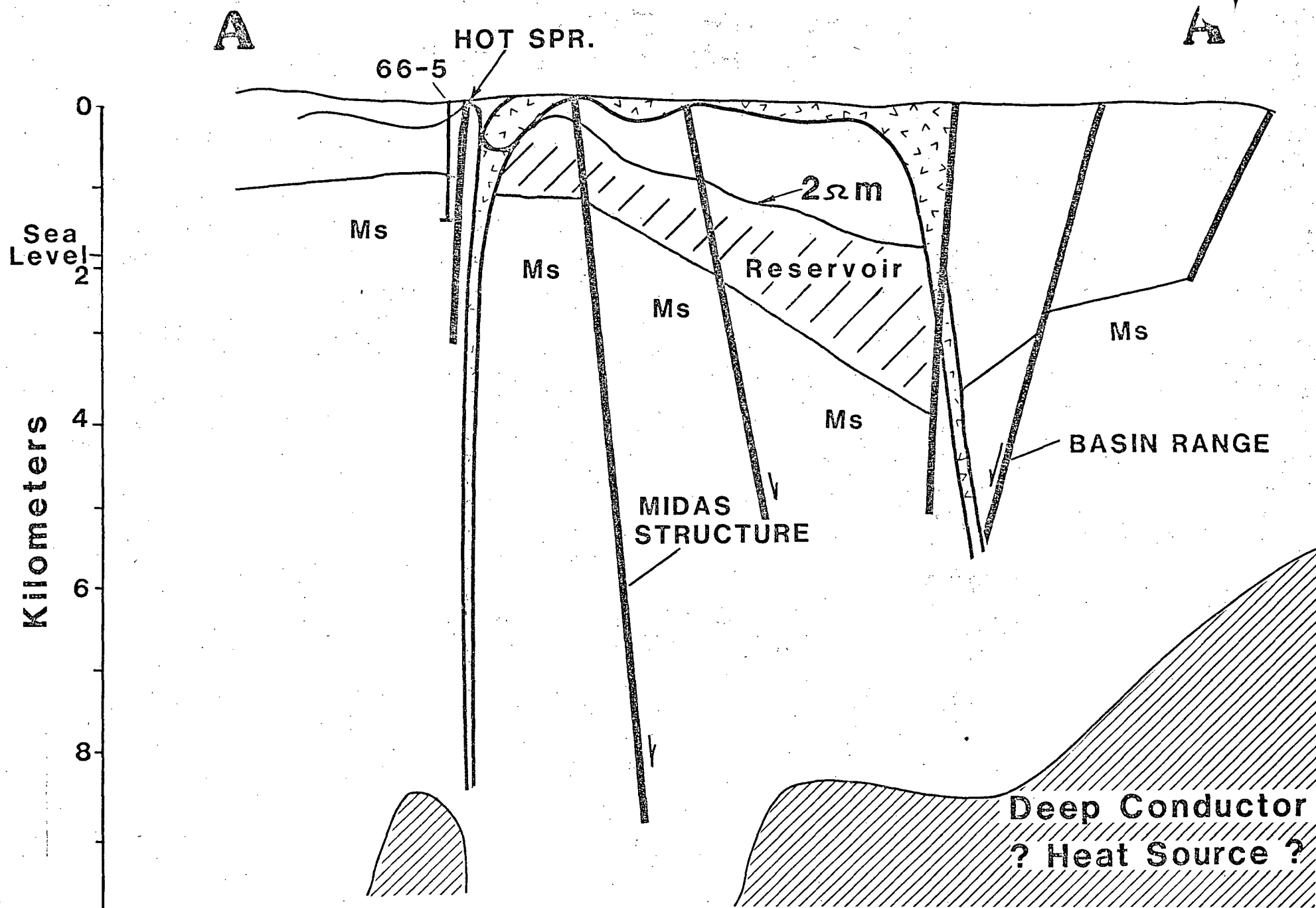


Figure 26L. Reservoir concept showing profile A-A' location.



GEOPHYSICAL SYNTHESIS & POSSIBLE RESERVOIR

Figure 27R. Geophysical synthesis and possible reservoir section along A-A'.